Eur. Phys. J. B **11**, 41–58 (1999)

THE EUROPEAN PHYSICAL JOURNAL B

EDP Sciences

Small bipolarons in the 2-dimensional Holstein-Hubbard model. I. The adiabatic limit

L. Proville[a] and S. Aubry[b]

Laboratoire Léon Brillouin (CEA-CNRS), CEA Saclay 91191-Gif-sur-Yvette Cedex, France

Received 10 December 1998

Abstract. The spatially localized bound states of two electrons in the adiabatic two-dimensional Holstein-Hubbard model on a square lattice are investigated both numerically and analytically. The interplay between the electron-phonon coupling g, which tends to form bipolarons and the repulsive Hubbard interaction $v \geq 0$, which tends to break them, generates many different ground-states. There are four domains in the g, v phase diagram delimited by first order transition lines. Except for the domain at weak electron-phonon coupling (small g) where the electrons remain free, the electrons form bipolarons which can 1) be mostly located on a single site (small v, large g); 2) be an anisotropic pair of polarons lying on two neighboring sites in the magnetic singlet state (large v, large g); or 3) be a "quadrisinglet state" which is the superposition of 4 electronic singlets with a common central site. This quadrisinglet bipolaron is the most stable in a small central domain in between the three other phases. The pinning modes and the Peierls-Nabarro barrier of each of these bipolarons are calculated and the barrier is found to be strongly depressed in the region of stability of the quadrisinglet bipolaron.

PACS. 71.10.Fd Lattice fermion models (Hubbard model, etc.) – 71.38.+i Polarons and electron-phonon interactions – 74.20.Mn Nonconventional mechanisms (spin fluctuations, polarons and bipolarons, resonating valence bond model, anyon mechanism, marginal Fermi liquid, Luttinger liquid, etc.) – 74.25.Jb Electronic structure

1 Introduction

The standard BCS theory of superconductivity [1] holds for a system of noninteracting electrons weakly coupled to a quantum field of phonons. It has been well-known for several decades that when the electron-phonon coupling increases too much, the BCS theory breaks down because of lattice instabilities [2]. As a consequence, rather low critical temperatures (≈ 30 K) were predicted as the upper bound for real BCS superconductors [3]. Many theories have subsequently been developed to describe the strong coupling regime with the hope to predict the existence of non-BCS superconductors with high critical temperature. After the discovery by Bednorz and Müller [4–6] of cuprate materials, which can be superconducting at temperatures as high as 100 K or more, the bipolaron approach (among others) regained much interest [7].

Since Landau [8], it has been acknowledged that a single electron (or equivalently a pair of noninteracting electrons coupled to a deformable classical field) may localize in the potential created self-consistently by a deformation of the field. The resulting object is called "polaron" for one electron or "bipolaron" for two electrons. The bipolaron theory of Alexandrov *et al.* [9] involves small bipolarons which are pairs of electrons with opposite spins, sharply localized at single sites of the lattice. Actually, because the phonons are quantum, these bipolarons are hard-core bosons that could condense in a superfluid state. For models in two dimensions and more, bipolarons exist only when the electron-phonon coupling is large enough [10], and they are always sharply localized as small bipolarons when the interactions are local. Thus, taking physically realistic parameters for the model, the effective mass of the bipolarons becomes so huge (quasi-infinite) that it seems quite unreasonable to expect the bipolarons to become superfluid at a non-negligible temperature. This aspect of the problem has been emphasized recently in reference [11]. However, the argument used by these authors was based on standard considerations that did not take into account the effect of mass reduction we shall discuss in this and a subsequent paper [17].

Indeed, in realistic physical models, the characteristic energy of the bare electrons is usually a few eV and is much larger than the phonon energies which is at most about a tenth of an eV. As a result, the quantum fluctuations of the phonons become generally negligible as soon as the electron-phonon coupling is strong enough to generate bipolarons. Then the potential interactions between the bipolarons are much larger than their quantum kinetic

[a] *Present address*: DAMTP Cambridge University, Cambridge, CB3 9EW, UK.

[b] e-mail: aubry@llb.saclay.cea.fr

energy. In that situation, the many bipolaron structures should be well described by an effective Ising pseudospin Hamiltonian, predicting an insulating Bipolaron Charge Density Wave at low temperature [12–14].

However, there might exist special and exceptional situations where the effective mass of the bipolarons is not quasi-infinite but becomes small enough so that they possibly condense into a superfluid state. The smaller the bipolaron mass is, the higher the critical temperature should be. As conjectured in references [15,16], this situation might be produced by a well-balanced interplay between the bare electronic kinetic energy, the electron-phonon coupling and the direct electron-electron repulsion. The aim of this paper is to study this interplay in the simplest Holstein-Hubbard (HH) model where these interactions are present.

This first paper is devoted to the study of a single bipolaron in the HH model in the adiabatic limit, assuming classical phonons. Obviously the assumption that there are no quantum phonon fluctuations does not allow superfluid states (with many electrons). In the next paper [17], the quantum phonon correction to the adiabatic case will be studied. There, it will be shown that in some regions of the parameter space, there is indeed a drastic reduction of the quantum bipolaron's effective mass due to quantum resonances between several almost degenerate adiabatic bipolaron structures. A large part of the scientific material of these two papers can be already found (in French) in the PhD dissertation of one of us [18].

Some numerical studies of the bipolarons in the one-dimensional adiabatic HH model, were already presented in reference [19] (as well as few preliminary studies in two dimensions). Bipolarons always exist in one-dimensional models as expected, but when the Hubbard term υ increases from zero, a first order transition occurs between the single site bipolaron (S0) and a bipolaron (S1) composed of two bounded polarons on two neighboring sites in a magnetic singlet state. It was observed that the classical mobility of the bipolaron (assuming the lattice dynamics is classical) was significantly enhanced in the vicinity of this transition. Owing to the presence of the Hubbard term, quite small bipolarons could become nevertheless highly mobile over hundreds of lattice spacings.

The behavior of the bipolaron in the two-dimensional case is quite different from the one-dimensional case. Although it does not describe precisely the CuO_2 planes of cuprates [6], it might exhibit similar features as more realistic models. In two-dimensional models with local interactions, the bipolarons exist only for a large enough electron-phonon coupling and are always sharply localized (small bipolarons). We numerically calculate these bipolarons by using a continuation method of these solutions from the anti-integrable limit [20], where the electronic transfer integral is zero.

The ground state of the bipolarons in this limit can be easily found and consists of either a bipolaron localized at a single site (S0) or of two uncoupled polarons at arbitrary different sites, but there are many other states with larger energy that are combinations of singlet states (multisinglets). Many of these bipolaron states can be continued when the transfer integral varies from zero and their energies can be compared. Although the bipolaron (S0) or the singlet bipolaron (S1), persist with the lowest energy in large parts of the phase diagram, it is found that a quadrisinglet state (QS) becomes the ground-state in an intermediate regime of parameters.

We show that we can reproduce quite accurately the same phase diagram by choosing variational wave functions for the electrons made from simple combinations of exponentials reproducing the main characteristic of the spin structure of the bipolaron. (This is an extension of the variational method used in Ref. [21]). Further extensions could be developed later for the many-body problem.

We investigate the properties of all the obtained solutions by calculating their binding energies, their pinning and breathing modes and also their Peierls-Nabarro energy barrier. We find a substantial softening of their pinning (and breathing) modes and a sharp depression of the PN energy barrier in the region where the (QS) bipolaron becomes the ground-state. Although the classical mobility of the bipolarons never becomes as large as in the one-dimensional case [19], it is sufficient to favor a good quantum mobility [17] in a specific region of the phase diagram.

2 The model

To keep in mind the physical magnitude of the dimensionless parameters involved in our reduced model, let us first write the Holstein-Hubbard Hamiltonian with all its parameters measured in the original physical units:

$$\mathcal{H} = -T \sum_{\langle i,j\rangle,\sigma} C^{+}_{i,\sigma} C_{j,\sigma} + \sum_i \hbar\omega_0 (a_i^{+} a_i) + \sum_i g n_i (a_i^{+} + a_i) + \sum_i \upsilon n_{i,\uparrow} n_{i,\downarrow}. \quad (1)$$

The electrons are represented by the standard fermion operators $C^{+}_{i,\sigma}$ and $C_{j,\sigma}$ at site i with spin $\sigma = \uparrow$ or $\downarrow$. Then T is the transfer integral of the electrons between nearest neighbor sites $\langle i,j\rangle$ of the lattice. In physical systems, its order of magnitude is usually measured in eV.

a_i^{+} and a_i are standard creation and annihilation boson operators of phonons. $\hbar\omega_0$ is the phonon energy of a dispersionless optical phonon branch with order of magnitude a tenth of an eV at most.

g is the constant of the on-site electron-phonon coupling which may physically range from zero to a fraction of an eV. The on-site electron-electron interaction is represented by a Hubbard term with positive coupling υ which may range physically from negligible to large values of the order of 10 eV.

Choosing $E_0 = 8g^2/\hbar\omega_0$ as the energy unit and introducing the position and momentum operators:

$$u_i = \frac{\hbar\omega_0}{4g}(a_i^{+} + a_i) \quad (2)$$

$$p_i = \mathrm{i}\frac{2g}{\hbar\omega_0}(a_i^{+} - a_i) \quad (3)$$

we obtain the dimensionless Hamiltonian:

$$H = \sum_i \left(\frac{1}{2}u_i^2 + \frac{1}{2}u_i n_i + U n_{i\uparrow} n_{i\downarrow}\right) - \frac{t}{2}\sum_{\langle i,j\rangle,\sigma} C^+_{i,\sigma} C_{j,\sigma} - \frac{\gamma}{2}\sum_i p_i^2. \quad (4)$$

The parameters of the system are now:

$$E_0 = 8g^2/\hbar\omega_0 \qquad U = \frac{\upsilon}{E_0} \qquad t = \frac{T}{E_0} \qquad \gamma = \frac{1}{4}(\frac{\hbar\omega_0}{2g})^4 \quad (5)$$

The parameter γ measures how "quantum" is the lattice. The BCS theory requires $g \ll \hbar\omega_0$: that is, large γ. We are interested in the opposite regime of strong electron-phonon coupling: that is, g larger than the phonon energy $\hbar\omega_0$. Then γ becomes small.

Thus the adiabatic approximation, which is simply obtained by taking $\gamma = 0$, becomes valid in the strong electron phonon regime. We shall assume this condition in this first paper. Then $\{u_i\}$ commutes with the Hamiltonian and can be taken as a scalar variable. For a given set of $\{u_i\}$, the adiabatic Hamiltonian

$$H_{\rm ad} = \sum_i \left(\frac{1}{2}u_i^2 + \frac{1}{2}u_i n_i + U n_{i\uparrow} n_{i\downarrow}\right) - \frac{t}{2}\sum_{\langle i,j\rangle,\sigma} C^+_{i,\sigma} C_{j,\sigma} \quad (6)$$

commutes with the total spin of the system.

Thus, the eigenstates of a system with two electrons are either nondegenerate singlet states or three-fold degenerate triplet states. The wavefunction of the singlet state has the form

$$|\Psi\rangle = \sum_{i,j} \psi_{i,j} C^+_{i,\uparrow} C^+_{j,\downarrow} |\emptyset\rangle \quad (7)$$

where $|\emptyset\rangle$ is the vacuum (no electrons in the system) and $\psi_{i,j} = \psi_{j,i}$ is normalized

$$\sum_{i,j} |\psi_{i,j}|^2 = 1 \quad (8)$$

on the $2D$ lattice $(\mathbb{Z}^D)^2$ ($D = 2$ being the lattice dimension we consider in this paper). The wave function of the triplet state (oriented with the spin $+1$ in order to fix the ideas), has the form

$$|\Psi\rangle_{\rm T} = \sum_{i,j} \psi^{\rm T}_{i,j} C^+_{i,\uparrow} C^+_{j,\uparrow} |\emptyset\rangle \quad (9)$$

where $\psi^{\rm T}_{i,j} = -\psi^{\rm T}_{j,i}$ is normalized and antisymmetric. Actually, the singlet wave and the triplet functions which are eigenstates of the adiabatic Hamiltonian (6) both yield the same eigen-equation for their components $\psi_{i,j}$ or $\psi^{\rm T}_{i,j}$

$$-\frac{t}{2}\Delta\psi_{i,j} + \left(\frac{1}{2}(u_i + u_j) + U\delta_{i,j}\right)\psi_{i,j} = F_{\rm el}(\{u_i\})\psi_{i,j} \quad (10)$$

where Δ is the discrete Laplacian operator in the 2D lattice $(\mathbb{Z}^D)^2$ defined as $(\Delta\Psi)_i = \sum_{j:i} \Psi_j$ where $j \in (\mathbb{Z}^D)^2$ are the nearest neighbors of $i \in (\mathbb{Z}^D)^2$.

Unlike the singlet states, the eigenenergies of the triplet states do not depend on the Hubbard term U since $\psi^{\rm T}_{i,i} = 0$ and thus are just the same as for noninteracting electrons. Taking into account that in our model, the transfer integrals with amplitude $t > 0$ connect only the nearest neighbor sites, it is straightforward to check that the singlet state defined as $\psi_{i,j} = |\psi^{\rm T}_{i,j}|$ always has less energy than the triplet state with wave function $\{\psi^{\rm T}_{i,j}\}$. As a result, the ground-state of our system is necessarily a singlet state with the form (7).

The energy of (6) depends on $\{\psi_{i,j}\}$ and $\{u_i\}$ as

$$F(\{\psi_{i,j}\},\{u_i\}) = \sum_i \left(\frac{1}{2}u_i^2 + \frac{u_i}{2}\rho_i + U|\psi_{i,i}|^2\right) - \frac{t}{2}\langle\psi|\Delta|\psi\rangle \quad (11)$$

where the electronic density at site i is

$$\rho_i = \sum_j (|\psi_{i,j}|^2 + |\psi_{j,i}|^2). \quad (12)$$

Extremalizing $F(\{\psi_{i,j}\},\{u_i\})$ with respect to the normalized electronic state $\{\psi_{i,j}\}$ and the displacements $\{u_i\}$ yields the set of coupled equations (10) and

$$u_i + \frac{\rho_i}{2} = 0. \quad (13)$$

$F_{\rm el}(\{u_i\})$ is an eigenenergy of two interacting electrons in the potential generated by the lattice distortion $\{u_i\}$. Using equation (13), the extrema of equation (11) are those of the variational energy

$$F_{\rm v}(\{\psi_{i,j}\}) = \sum_i \left(-\frac{1}{8}\rho_i^2 + U|\psi_{i,i}|^2\right) - \frac{t}{2}\langle\psi|\Delta|\psi\rangle \quad (14)$$

for $\psi_{i,j}$ normalized and where ρ_i is given by equation (12). Then, it follows that

$$-\frac{t}{2}\Delta\psi_{i,j} + \left(-\frac{1}{4}(\rho_i + \rho_j) + U\delta_{i,j}\right)\psi_{i,j} = F_{\rm el}\psi_{i,j} \quad (15)$$

and also that for the solutions of this equation, the energy of the system is

$$F_{\rm v}(\{\psi_{i,j}\}) = F_{\rm el} + \frac{1}{8}\sum_i \rho_i^2. \quad (16)$$

3 Numerical continuations of bipolarons from the anti-integrable limit

3.1 Bipolarons in the anti-integrable limit

In the anti-integrable limit $t = 0$, the adiabatic ground-state for two electrons is easily found. For $U \leq 1/4$, it

consists of a pair of electrons localized at a single site i. This is the standard small bipolaron known in the literature, denoted (S0) (see Fig. 1). For a bipolaron at site i, its electronic wave function is

$$|\Psi\rangle = C^+_{i,\uparrow} C^+_{i,\downarrow} |\emptyset\rangle \tag{17}$$

and its energy is $F_{\rm v} = U - 1/2$.

When $U \geq 1/4$, the ground-state consists of two unbound polarons localized at arbitrary different sites i and j and with arbitrary spins. It is thus degenerate and its energy $F_{\rm v} = -1/4$ is independent of the Hubbard interaction. When sites i and j are nearest neighbors, we define the bipolaron (S1) [15,16] (see Fig. 1) with electronic wave function

$$|\Psi\rangle = \frac{1}{\sqrt{2}} (C^+_{i,\uparrow} C^+_{j,\downarrow} + C^+_{j,\uparrow} C^+_{i,\downarrow}) |\emptyset\rangle \tag{18}$$

where i and j are nearest neighbor sites.

Since a single polaron has the electronic spin 1/2, when the transfer integral t is small but not zero, a standard perturbation theory yields an antiferromagnetic exchange coupling $2t^2/U$ between the two spins of the uncoupled neighboring polarons. When the spins are chosen in the singlet state represented by equation (18), these two polarons have the energy $F_{\rm v} \approx -1/4 - t^2/U$. When they are not located at nearest-neighbor sites but at the lattice distance n, perturbation theory to order n yields an antiferromagnetic exchange coupling proportional to $U(t/U)^{2n}$. Thus, for $t \ll U$, the minimum energy is obtained for nearest neighbor bipolarons in the singlet magnetic state (S1). It is maximum when U is close to and above 1/4, just when (S1) becomes of lower energy than (S0). For t fixed, it decreases to zero when U increases. This binding energy also vanishes in the anti-integrable limit t. Unlike bipolaron (S0), bipolaron (S1) breaks the square lattice symmetry and is oriented either in the x direction or the y direction.

When t is not very small, the spatial extension of the polarons goes significantly beyond single sites, and it is not obvious that a low-order perturbation theory holds. The true ground state might not be obtained by continuation of the solutions (S0) or (S1). There are infinitely many other bipolaron states at $t = 0$ (solutions of Eq. (10)), which have been classified in Appendix A[1]. Some of them are not very different in energy and could compete to become the true bipolaron ground-state when t increases. Therefore, it becomes useful to test the ground-state of the bipolaron at $t \neq 0$ among the extrema of equation (14) that are obtained by continuation from those calculated in the anti-integrable limit at $t = 0$.

It is of course impossible to continue and to test numerically the energy of all the solutions of equation (10) at $t = 0$. The study of Appendix A shows that the binding energy of the bipolarons is non-negligible only when the total number N_s of occupied sites is not too large. The non-connected bipolaron states are discarded because at $t = 0$ they always have more energy than their connected component with the smallest energy, and at $t \neq 0$, their absence of connectivity is not favorable for gaining energy from the electronic kinetic energy term with amplitude t.

On the contrary, the star multisinglet bipolaron states with one central site with electronic density $\rho_1 = 1$ ($N_1 = 1$) and $N_2 \leq 4$ nearest neighbor sites with electronic density $\rho_2 = 1/N_2$ and energy $F_{\rm v} = -(1+1/N_2)/8$ at $t = 0$ appear much more favorable for reducing their energy when t increases. They are still spatially well-localized, which allows an efficient energy gain from the electron phonon coupling and only a small energy loss due to the Hubbard term (no doubly occupied sites). Moreover, the peripheral electron can gain a substantial electronic kinetic energy by occupying N_2 sites when $N_2 > 1$. In the limit of N_2 large, this energy gain can reach a maximum at $2t$. These bipolaron states have no continuous degeneracy at $t = 0$ and thus according to the implicit function theorem, they can be continued for t not too large.

At $t = 0$, the electronic wave function of a star N_2-singlet bipolaron centered at the origin 0 is:

$$|\Psi\rangle = \sum_{\nu} \frac{1}{\sqrt{2N_2}} (C^+_{0,\uparrow} C^+_{j_\nu,\downarrow} + C^+_{j_\nu,\uparrow} C^+_{0,\downarrow}) |\emptyset\rangle \tag{19}$$

where j_ν are neighboring sites to the origin. They could also be chosen farther away, but when the bipolaron becomes too extended, its energy does not decrease sufficiently to become the ground-state. We tested the most compact bipolarons which are star bisinglet bipolaron states (BS) with $N_2 = 2$ and j_ν are the two neighboring sites to the origin in the direction x (or x and y), star trisinglet bipolaron states (TS) where N_2=3 and j_ν are three of the neighboring sites of the origin, and the square symmetric quadrisinglet (QS) ($N_2 = 4$) which involves the four neighboring sites of the origin.

For larger or infinite lattices, multisinglets with equal electronic densities at the occupied sites might not be too high in energy and have been also tested. Although they are continuously degenerate in the anti-integrable limit, their degeneracy is raised when $t \neq 0$. We considered for example, the square symmetric quadrisinglet state (QS2) which occupies the four corners j_ν of an elementary square of the lattice. One of its degenerate wave functions is

$$|\Psi\rangle = \sum_{\nu \neq \nu'} \frac{1}{\sqrt{8}} C^+_{j_\nu,\uparrow} C^+_{j_{\nu'},\downarrow} |\emptyset\rangle \tag{20}$$

with energy $F_{\rm v} = -1/8$

3.2 Numerical technique of continuation

The most efficient numerical techniques for the continuation of solutions of sets of equations as a function of a parameter, are usually based on a Newton method. For example, such techniques were developed efficiently for calculating discrete breathers [23]. In our case to calculate

[1] Actually, this result should not be surprising since there are already infinitely many metastable states in addition to the standard single bipolaron [22] (see also Sect. 5.4 in Ref. [13]) in the pure Holstein model, which however never become ground-state.

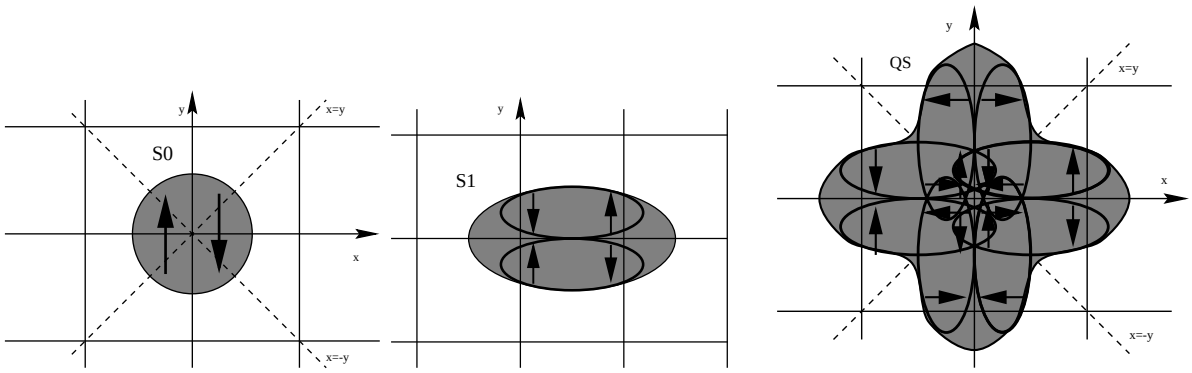

Fig. 1. Schemes of the bipolarons (S0), (S1) and (QS) appearing as possible ground-states

accurately adiabatic bipolarons on a 2D system, a reasonable size should be 10×10. Then calculating the 10^4 components of $\psi_{i,j}$ with a Newton method, requires to work with huge matrices containing 10^8 coefficients: that is, to use a large-memory, fast computer. Actually, smaller size conventional computers suffice if one uses appropriate techniques needing a much smaller working space. This technique does not allow to continue all solutions but only those which are locally stable (in particular, the bipolaron ground-state) and those that can be made stable by fixing some spatial symmetries of the bipolaron.

This method is quite simple in its principle. To solve equation (15) with condition (12), we start from a normalized trial solution of equation (15), $\Phi = \{\phi_{i,j}\}$ with $\phi_{i,j} = \phi_{j,i}$, and we calculate recursively a new normalized trial solution $\Psi_1 = \mathcal{T}(\Phi) = \{\psi_{i,j}\}$ as

$$\mathcal{N}_1 \psi_{i,j} = -\frac{t}{2} \Delta\phi_{i,j} + \left(U\delta_{i,j} - \sum_k (\phi_{i,k}^2 + \phi_{j,k}^2) - K \right) \phi_{i,j} \tag{21}$$

where $\mathcal{N}_1$ is the normalization factor (chosen negative) and K is some positive constant that we introduce to ensure the convergence to a minimum energy state. Actually, it can be chosen to be zero in the domain of parameter we study.

We find numerically that for n large enough, $\Psi_n = \mathcal{T}(\Psi_{n-1})$ and its normalization factor $\mathcal{N}_n$ converge to the limits Ψ and $\mathcal{N}$, respectively. Ψ is a solution of equation (15) with the condition (12) and for the eigenenergy $F_{\rm el} = \mathcal{N} - K$. This solution corresponds to the eigenvector of equation (15) (where ρ_i and ρ_j are fixed) associated with the eigenvalue $F_{\rm el}$ which is such that $F_{\rm el} - K$ has the largest modulus. In principle, the constant K is chosen large enough in order that $F_{\rm el}$ is surely the lowest negative eigenvalue: that is, for the electronic ground-state. One can easily check in the anti-integrable limit that $K = 0$ is an appropriate choice when $U < 1/2$. Varying one of the model parameters by small steps, each solution is taken as a trial solution for the next step. It is easy to determine whether the solution varies quasicontinuously or discontinuously.

For the solutions in the anti-integrable limit which are non-degenerate, it can be checked that the hypotheses of the implicit function theorem, are fulfilled. Thus continuation is in principle possible[2]. For those which belong to a degenerate continuum, the conditions for applying the implicit theorem are not fulfilled, but when some spatial symmetries or some constraints on the solution are fixed, the degeneracy at $t = 0$ can lifted and this theorem applies.

In the anti-integrable limit, only (S0) for $U < 1/2$ and (S1) for $0 < U$ (and (Sn) with $n > 0$ being the distance between two polarons) are numerically stable: that is, can be followed continuously from $t = 0$ by using algorithm (21). Actually, we choose as initial solution at $t = 0$, the exact bipolaron solutions described above, which are (S0), (S1), (QS), (BS), (TS) and (QS2). Maintaining by force the spatial symmetries of the solution at $t = 0$, the convergence process becomes stable again, and the continuation of these solutions is feasible.

The main advantage of our method is that it can be performed on standard computers. Its flaw is that we might not be able to follow continuously a solution that is mathematically continuable. Actually, rather few bipolaron states are continuable. In contrast, our method is very reliable for finding the true bipolaron ground state, because it brings spontaneously the bipolaron solution to a local minimum of the variational energy.

Actually, we checked that when there is no symmetry constrains and independent of the initial trial solution, in most cases our numerical algorithm converges spontaneously toward the same bipolaron state, which then can be considered as the true bipolaron ground-state. However, this situation does not occur in the vicinity of the first order transition lines where we can obtain a few different bipolaron states depending on the initial condition, but then their energies can be easily compared to find the ground-state.

[2] The implicit function theorem was already used in similar anti-integrable limits, for example in reference [24] for polarons and bipolarons in the original Holstein model or in reference [25] for discrete breathers.

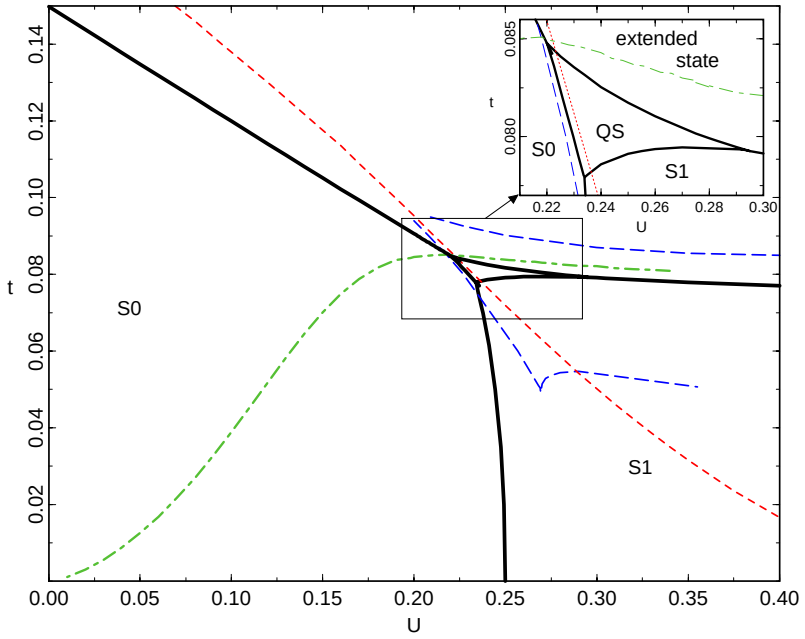

Fig. 2. Phase diagram of the bipolaron in the 2D Holstein-Hubbard model in the plane of parameters U and t. There are four phase domains separated by first order transition lines corresponding to bipolarons (S0), (S1), (QS) and two unbound extended electrons. Also shown are the limit of metastability of the bipolaron (S0) (dotted line), bipolaron (S1) (dot-dashed line) and bipolaron (QS) (dashed line). Insert: Magnification of the phase diagram around the triple point involving phases (S0), (S1) and (QS).

3.3 Bipolaron phase diagram

The ground-state for a pair of electrons is obtained by comparing the energies $F_{\rm v}$ of many bipolarons continued from the anti-integrable limit (see also [19]). For larger t, the ground-state corresponds to a pair of electrons extended over the whole system. There is a first order transition line, when t becomes smaller, at which the two electrons bind with each other and self-localize into a bipolaron. The region below this line is divided into three domains separated by other first-order transition lines. For U small, the bipolaronic ground-state is (S0). When U increases for t not too large, there is a transition line between bipolarons (S0) and (S1). For larger t, this transition line bifurcates at a triple point at $t \approx 0.785$ and $U \approx 0.235$ into two first order transition lines which both join the transition line with the extended states. In between the fork that is generated, there is a small domain where the bipolaron (QS) that was initially unstable for t small, recovers its stability and even becomes the ground-state. Other bipolaronic structures continued from the anti-integrable limit at $t = 0$ appear as minimum energy states in the domain shown in Figure 2. The (QS) solution can be viewed as a localized RVB state similar to that proposed by Anderson some years ago [26] in the pure Hubbard model in 2D as a theory for superconductivity in cuprates.

In our model, this (QS) bipolaron has the quantum symmetry (s) because the kinetic energy term is Laplacian-like. However, the study of Appendix C in the anti-integrable limit, suggests that it is close in energy to other states with quantum symmetry (s') or (d). Such symmetries could be favored by slight model variations on the form of the kinetic energy.

At the triple point, the bipolaronic structure of our model is degenerate between three states (S0), (S1) and (QS). Figure 3 shows the profiles of the electronic density for these three types of bipolaron, which have the same energy. Interestingly, they extend significantly over only a few sites, and thus can be called *small bipolarons*.

The binding energy of a bipolaron is defined as the difference between the smallest energy state where the pair of electrons is unbound, and the bipolaron energy. Depending on the parameters, this unbound state could be either two extended electrons with opposite spins in the plane wave state at zero momentum or two polarons localized far apart. The variation of this binding energy *versus* U and for several values of t is shown Figure 4.

At the triple point, the binding energy of the degenerate bipolarons (in that case, to produce two extended electrons) is much smaller than the binding energy of bipolaron (S0), at the same value of t but at $U = 0$. However, it still has a substantial value that is physically far from being negligible.

The binding of bipolarons (S1) and (QS) are physically better interpreted as being of magnetic origin. These bipolarons can be viewed as two closely bound polarons with spins 1/2. Their binding energy is mostly due to the spin energy gain obtained by lifting the spin degeneracy as a singlet state.

In the vicinity of the triple point and specifically in that region, the quantum lattice fluctuations ($\gamma \neq 0$) will also lift the degeneracy between the three degenerate

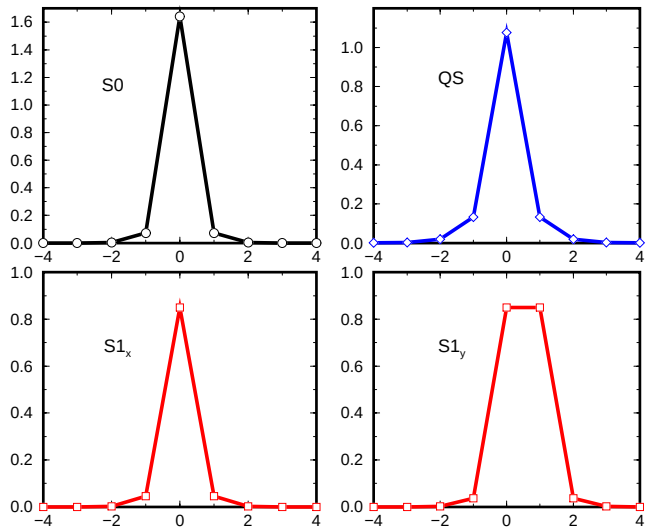

Fig. 3. Profile of electronic density versus site i at the triple point $t = 0.0779$, $U = 0.234$ for bipolarons (S0), (QS) and (S1) along their symmetry y-axis and the transverse x-axis. These three bipolarons have the same energy.

bipolarons (S0),(S1) (in both directions x and y), (QS) resulting in a sharp mass reduction (or equivalently a large tunneling energy or a large band width) (see [17]).

4 Variational calculation of bipolarons

We now reproduce, with good accuracy, the phase diagram shown in Figure 2 using simple variational approximations for the bipolarons (S0), (S1) and (QS). For that purpose, the variational forms have to be chosen appropriately under two conflicting constraints. On the one hand, they should be physically realistic enough in order to mimic the real ground-state. On the other hand, the analytical calculations of their variational energy should be practically feasible.

In reference [21], it was shown that an exponential form centered at the occupied site with a unique variational parameter, was a good variational form for a single polaron, reproducing accurately its quantitative properties. We choose a similar normalized variational form for the electronic wave function of bipolaron (S0) located at the origin

$$\psi^{\mathrm{S0}}_{i,j} = A\lambda^{(|i|+|j|)} \text{ with } A = \left(\frac{1-\lambda^2}{1+\lambda^2}\right)^2 \qquad (22)$$

(for $i = (i_x, i_y)$, we set $|i| = |i_x| + |i_y|$). This variational form is easily extended to the electronic wave function of bipolaron (S1) in a singlet magnetic state located at sites $(0,0)$ and $(1,0)$:

$$\psi^{\mathrm{S1}}_{i,j} = \frac{B}{\sqrt{2}}(\lambda^{(|i_x-1|+|i_y|+|j_x|+|j_y|)} + \lambda^{(|i_x|+|i_y|+|j_x-1|+|j_y|)})$$
$$\text{with} \quad B = \frac{(1-\lambda^2)^2}{(1+\lambda^2)\sqrt{1+6\lambda^2+\lambda^4}}. \qquad (23)$$

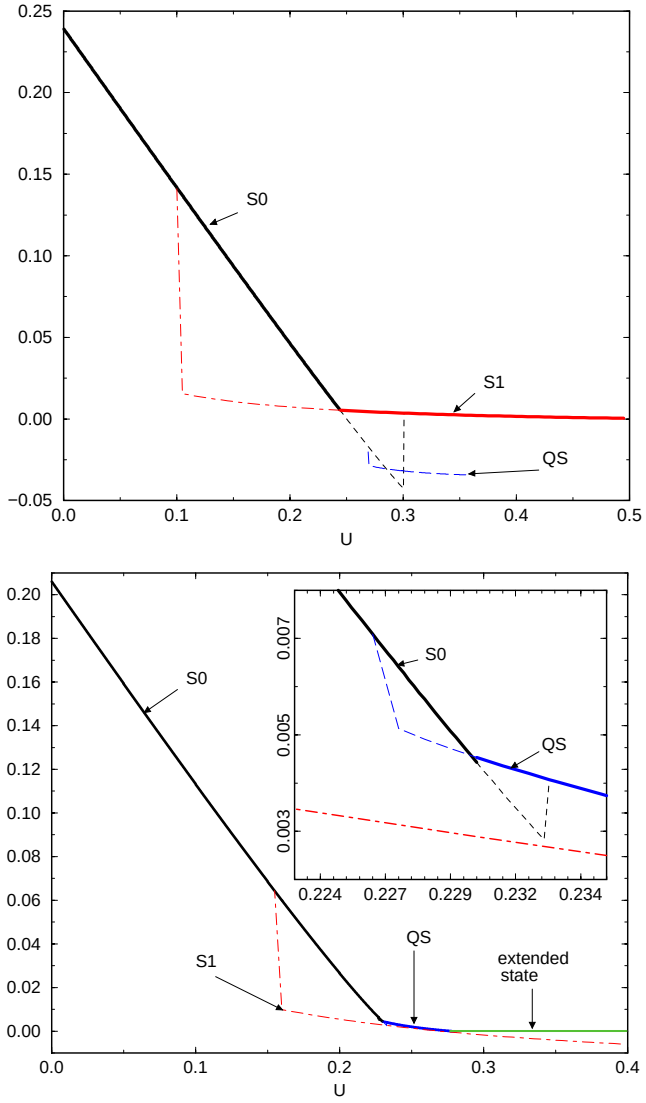

Fig. 4. Binding energy *versus* U of bipolaron (S0) (thin dotted line), (S1) (thin dot-dashed line) and (QS) (thin dashed line) at $t = 0.05$ (top) (compared to two remote polarons) and $t = 0.08$ (bottom) compared to two extended polarons. The upper envelope (thick line) is the binding energy of the ground-state. Insert: magnification at the first order transition between (S0) and (QS).

The variational form for the electronic wave function of bipolaron (QS) centered at the origin is a combination of four of these variational forms in the four directions of the square lattice, but now it becomes useful to introduce two variational parameters λ and μ instead of only one, to distinguish between the spatial extension of the polaron that is at the center from those that are the periphery:

$$\psi^{\mathrm{QS}}_{i,j} = \frac{C}{\sqrt{8}}\mu^{(|j_x|+|j_y|)}\sum_{\pm}(\lambda^{(|i_x\pm1|+|i_y|)} + \lambda^{(|i_x|+|i_y\pm1|)})$$
$$+ \frac{C}{\sqrt{8}}\mu^{(|i_x|+|i_y|)}\sum_{\pm}(\lambda^{(|j_x\pm1|+|j_y|)} + \lambda^{(|j_x|+|j_y\pm1|)}) \qquad (24)$$

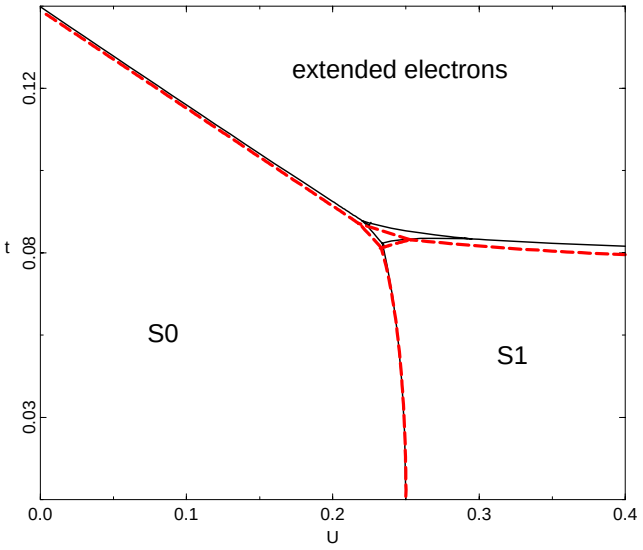

Fig. 5. Comparison between the exact phase diagram Figure 2 (thick lines) and its approximate calculation (dashed lines) Section 4.

where for normalization

$$C^{-2} = \left(\frac{1+\mu^2}{(1-\mu^2)(1-\lambda^2)}\right)^2 \times \left[(1+\lambda^2)^2 + \lambda^2(3-\lambda^2)(1+\lambda^2) + 8\lambda^2\right] + 4\frac{(1+\lambda\mu)^2(\lambda+\mu)^2}{(1-\lambda\mu)^4}. \quad (25)$$

The energy (14) can be analytically calculated with the variational forms (22, 23, 24). Extremalizing the resulting energy with respect to the parameters λ and μ yields the energies of bipolarons (S0), (S1) and (QS) with a very good accuracy. We do not reproduce here these tedious calculation. We also remark that this variational method allows one to compute the bipolaron structures even when they become unstable so that they cannot be numerically continued with our method. Comparing these variational energies allows one to produce a phase diagram that is very close to the exactly calculated one (see Fig. 5).

However, it is worthwhile to mention that the variational form (24) of bipolaron (QS) may yield some artefacts which are not found in the exact numerical calculations (as often occurs in variational calculations). Fortunately, they occur in parameter regions where this solution is not the ground-state, and thus do not affect the phase diagram. First, there is a first order transition of λ and μ near the anti-integrable limit. Second, there is another anomaly when increasing U. It is found that ψ^{QS} bifurcates onto a unbound solution where $\mu = 1$. This corresponds to an unbound pair of electrons in the spin singlet state where one electron is self-localized as a polaron and the second one is extended. As a result, the validity of the exponential form ψ^{QS} is limited to the (QS) region, that is when this bipolaron is the ground-state.

5 Internal modes and peierls nabarro barriers

The phonon frequencies of the bipolaron can be easily calculated within the standard Born-Oppenheimer approximation (in units $\sqrt{\gamma}$) as explained in [19]. It is found that the bipolarons exhibit several localized (or internal) modes. The breathing mode has the same symmetry as the bipolaron. The pinning modes are spatially antisymmetric and tend to move this bipolaron either in the x direction or the y direction. Figure 6 shows the variations of their frequencies with U. It is found that in the region of the triple point where three bipolaronic structures are almost degenerate, both the breathing and the pinning modes, soften significantly (approximately by a factor 2).

These weak frequencies for the internal modes can be considered as evidence that the self consistent potential in which the bipolaron is pinned becomes rather flat, which means a small Peierls Nabarro barrier (PN). It is thus useful to calculate precisely this PN energy barrier in order to confirm this conjecture. In addition, it is found that the paths that yield the lowest PN energy barrier vary in the parameter space. The several ways to move the bipolaron are sometimes almost equivalent in energy. These paths should play a role in the quantum tunnelling of the bipolarons

The PN energy barrier is the minimum energy that must be provided to the bipolaron to move it by one lattice spacing. For that we have to determine a continuous path of bipolaronic configurations which connects the initial bipolaron to a shifted equivalent bipolaron. There is a maximum of energy along any path, and the minimum over all paths of this maximum (called minimax) yields the PN energy barrier.

To move a bipolaron with electronic wave function $\{\psi^i_{n,m}\}$ from site i to a neighboring site j (where $\{\psi^j_{n,m}\} = \{\psi^i_{n+j-i,m+j-i}\}$), we consider a continuum of bipolaronic solutions $\{\psi_{n,m}(c)\}$ which depend on c for $c_0 \leq c \leq c_1$, and such that $\{\psi_{n,m}(c_0)\} = \{\psi^i_{n,m}\}$ and $\{\psi_{n,m}(c_1)\} = \{\psi^j_{n,m}\}$.

It is convenient for simplicity to choose as variable $c(\Psi)$, one of the bipolaron components or a simple function of them. For any continuous path that connects the bipolaronic ground-state $\Psi^i = \{\psi^i_{n,m}\}$ at site i to the same configuration $\Psi^j = \{\psi^j_{n,m}\}$ at an equivalent neighboring site j, c must take all the values between $c_0 = c(\Psi^i)$ to $c_1 = c(\Psi^j)$. For each value of c, the energy of the bipolaronic state will be always larger than or equal to the minimum of energy of the bipolaronic configuration where the component corresponding to $c(\Psi)$ is fixed to c. Thus, starting from the initial ground-state configuration, and following continuously this minimum by varying this constraint c, we may pull continuously the bipolaron from one site i to its neighboring site j.

For that purpose, the choice of $c(\Psi)$ has to be appropriate to obtain a path of bipolaronic configurations that connects *continuously* the two bipolaronic configurations Ψ^i and Ψ^j and that yields the lowest minimax. We guess intuitively that the bipolaron could be effectively pulled only if this constraint affects the "main body" of the

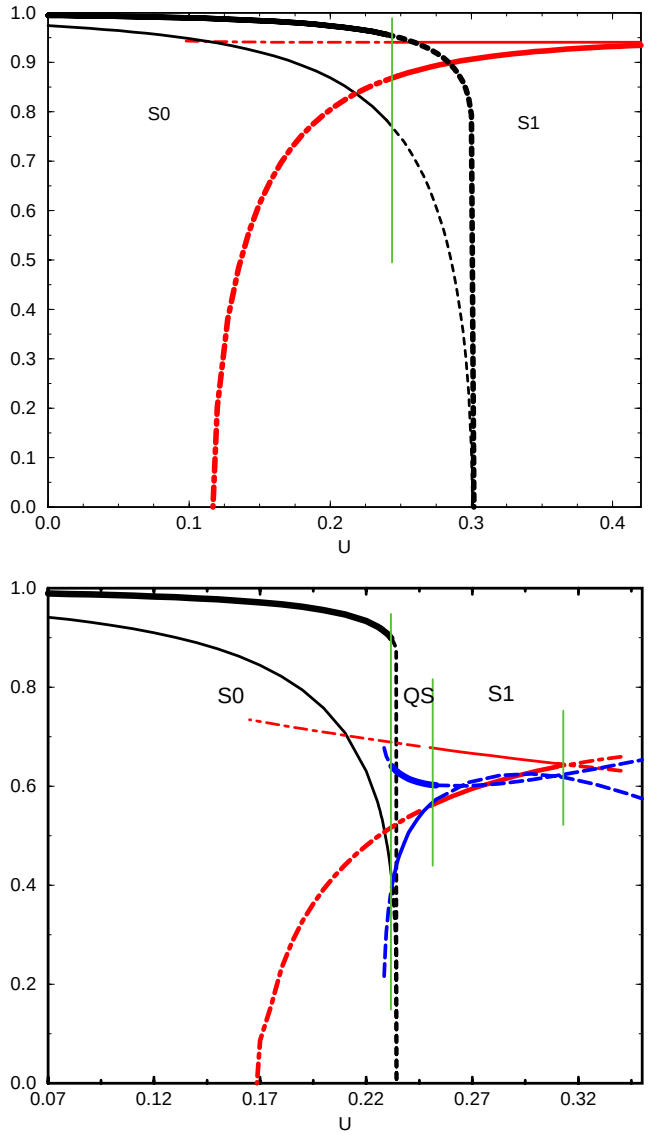

Fig. 6. Phonon frequencies *versus* U of the pinning mode (thick line) and breathing mode (thin line) for bipolaron (S0) (dotted line), bipolaron (S1) (dot-dashed line), bipolaron (QS) (dashed line) at $t = 0.05$ (top) and $t = 0.08$ (bottom). When, these bipolarons are ground-state, the corresponding lines are plain. Vertical lines indicate the first order transitions.

bipolaron instead of a minor component. For our investigations, we found several continuous paths of configurations competing for providing the minimax. We obtain them by using several kinds of constraints for a bipolaron at site i moving to site j which may be:

$$\psi_{i,i} = c \tag{26}$$
$$\psi_{i,j} = \psi_{j,i} = c \tag{27}$$
$$\psi_{j,k} = \psi_{k,j} = c \tag{28}$$
$$\psi_{i,i} - \psi_{j,j} = c \tag{29}$$

($k \neq i$ is a neighboring site of j and bond $j - k$ could be either collinear with or orthogonal to bond $i - j$). These constraints c are easily taken into account with few minor changes in the numerical programs described above minimizing the variational form (14). When $\psi_{i,i}$, $\psi_{i,j}$ or $\psi_{j,k}$ is fixed to c, it suffices to drop the corresponding equation (15). When $\psi_{i,i} - \psi_{j,j} = c$, it is convenient to define the new variable $\phi = (\psi_{i,i} + \psi_{j,j})/\sqrt{2}$. Then, the variational form (14), depends on ϕ, c and $\psi_{n,m}$ for $(m,n) \neq (i,i)$ and $\neq (j,j)$. The vector with components ϕ and $\{\psi_{m,n}\}$ (with $(m,n) \neq (i,i)$ and $\neq (j,j)$), has norm $\sqrt{1 - c^2/2}$ which is fixed by the constraint c. Extremalizing (14) with respect to its free variables yields a set of equations that differ slightly from (15), although they depend on c as a parameter. They can be solved with the same iterative method as before.

We may thus obtain a continuous path of configurations parameterized by c and connecting the bipolaron ground-state to the same state shifted by one lattice spacing. The extrema of the energy $F_v(c)$ given by (14) (which satisfy $\partial F_v(c)/\partial c = 0$) correspond to bipolaronic solutions without constraint. Actually, they can be identified among the bipolarons that are classified in Appendix A. When one of these bipolaron is found spatially symmetric with a symmetry center at the middle of the bond $\langle i,j \rangle$, there is no need to continue the path beyond this point because it is clear that it can be completed by symmetry. We test the different constraints (29) and among those that yield a continuous path, the lowest maximum is considered as the minimax.

The PN energy barrier is then the difference between the minimum of energy and the maximum along this best continuous path.

When the PN energy barrier is smaller than or at most comparable to the binding energy of the bipolaron, the two polarons remain surely bound during their continuous lattice translation and it is then reasonable to believe that the minimax obtained with the above method is correct. However, there are regions in the parameter space where this condition is not fulfilled, and a precise determination of this PN energy barrier might be questionable. In any case, the obtained value, if not exact, is necessarily an overestimate.

When (S0) is the ground-state and U is not too large, the energy variation *versus* $c = \psi_{i,i} - \psi_{j,j}$ starting from the ground-state bipolaron (S0) is shown in Figure 7. This path does not need to be continued beyond the point $c = 0$ because it exhibits a minimax at $c = 0$ corresponding to a spatially symmetric bipolaron and thus can be completed by symmetry. This bipolaron has only one unstable mode and is the continuation at U small of the stable bipolaron (S1) beyond its bifurcation point. At $U = 0$, its electronic state corresponds to two electrons with opposite spins in the lowest eigenstate of the potential generated by the lattice distortion (Slater determinant). The analysis of Appendix B suggests that for $U < 0$, this bipolaron can be continued as the two-site bipolaron (2S0) in the anti-integrable limit.

When U becomes larger, the previous constraint does not always yield a continuous path, and another constraint $\psi_{i,j} = c$ is found efficient for providing a continuous path with a minimax. The energy variation *versus* $c = \psi_{i,j}$

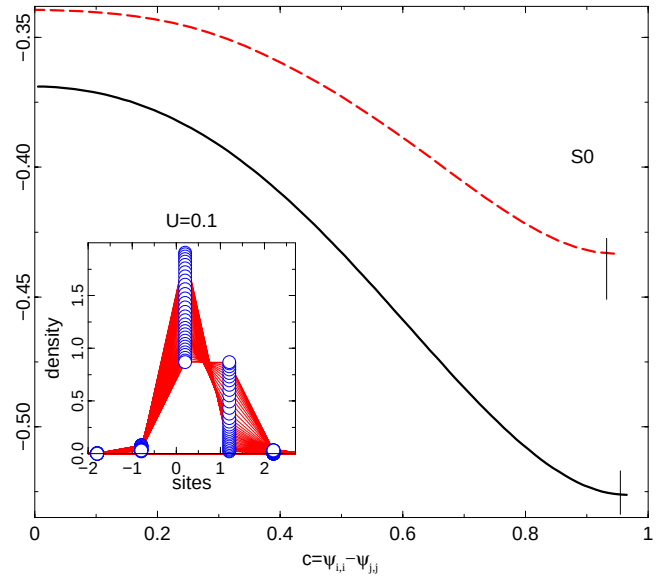

Fig. 7. Energy variation *versus* c of the bipolaronic ground-state state under the constraint $\psi_{i,i} - \psi_{j,j} = c$. Bipolaron (S0) is initially at site i and j is the neighboring site towards which this bipolaron moves. $t = 0.08$ and $U = 0$ (plain line), $U = 0.1$ (long dashed line). Vertical lines indicate the location of the energy extrema corresponding to the initial bipolaron (S0). Insert: Variation of the profile of electronic density along the continuous path of the bipolaron at $t = 0.08$, $U = 0.1$.

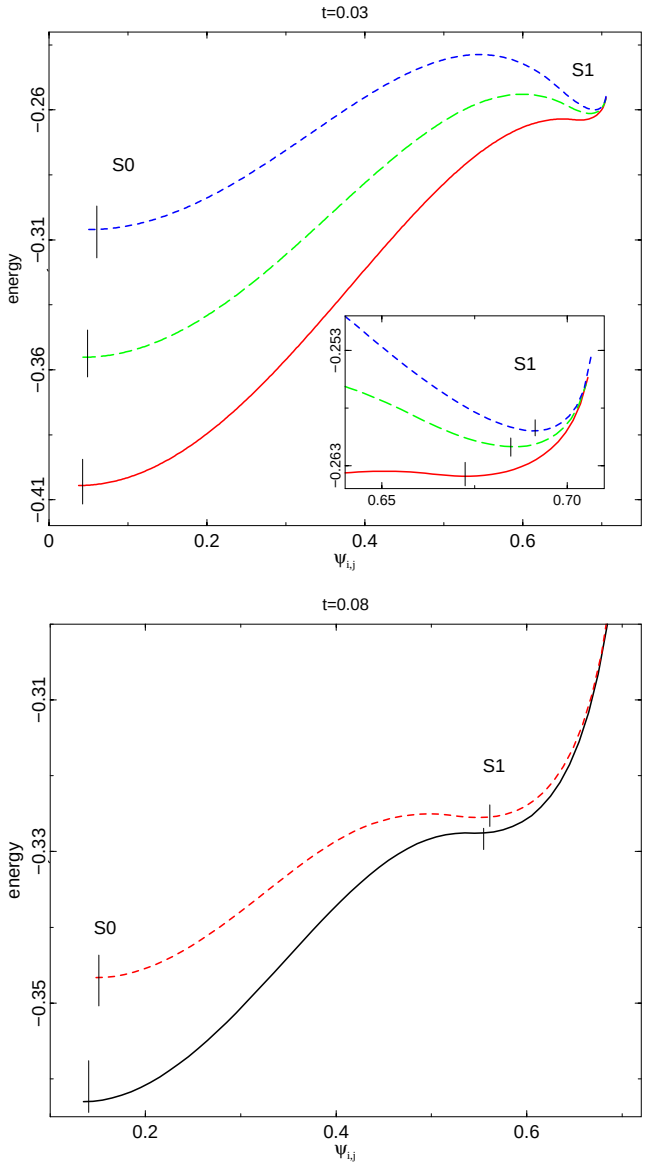

Fig. 8. Same as Figure 7 but with the constraint $\psi_{i,j} = c$ and different parameters. top: $t = 0.03$, $U = 0.1$ (full line), $U = 0.15$ (long dashed line), $U = 0.2$ (dashed line) insert: magnification bottom: $t = 0.08$, $U = 0.18$ (full line), $U = 0.2$ (dashed line). Vertical lines indicates the location of the energy extrema corresponding to bipolaron (S0) and to bipolaron (S1).

starting from the ground-state bipolaron (S0) is shown in Figure 8 for some bipolarons. We observed that in addition to the minimum (S0), it exhibits two other extrema. The second minimum corresponds to the spatially symmetric bipolaron (S1). Again, there is no need to construct a complete path reaching (S0), since this path can be completed by symmetry. This figure shows that a pitchfork bifurcation occurs for the minimax when U increases from zero (at fixed t). The unstable bipolaron (2S0) bifurcates into a minimum corresponding to the stable bipolaron (S1) and two symmetric minimax corresponding to intermediate unstable bipolarons (with one unstable mode), which are nothing but the star sister bipolarons (S1/S0) described in Appendix A.2[3]. Actually, this bifurcation line between (S1/S0) and (S1) appears in Figure 2 as the left border line of the domain of metastability of bipolaron (S1). In that regime, the motion of the bipolaron involving the minimum energy consists in first stretching bipolaron (S0) into bipolaron (S1) along one lattice direction, and next in squeezing this bipolaron in the same direction to recover the bipolaron (S0) translated by one lattice spacing. This feature is identical to those found for the two-site model in Appendix B.

When bipolaron (QS) (which does not exist for the two-site model) becomes the ground-state instead of (S0), the PN energy barrier should be studied from this initial configuration. Figure 9 shows the energy variation *versus* $\psi_{i,j} = c$ starting from bipolaron (QS). The continuous path exhibits another minimum corresponding to the stable bipolaron (S1), which is spatially symmetric. Again, the continuous path can be completed by symmetry. There is a minimax which correspond to another bipolaronic configuration, which we did not analyze in detail but is likely to be the star trisinglet denoted (TS) described in Appendix A.1. This curve also demonstrates that for this value of t, the bipolaronic ground-state changes by a first-order transition from (QS) to (S1) when increasing U.

It is also worthwhile to note that there is also a PN energy barrier between the bipolaron (S0) and (QS), which

[3] It is worthwhile to note a similar phenomenon observed when narrow discrete breathers become mobile [27]. Intermediate discrete breathers breaking the lattice symmetry were also found to appear [28].

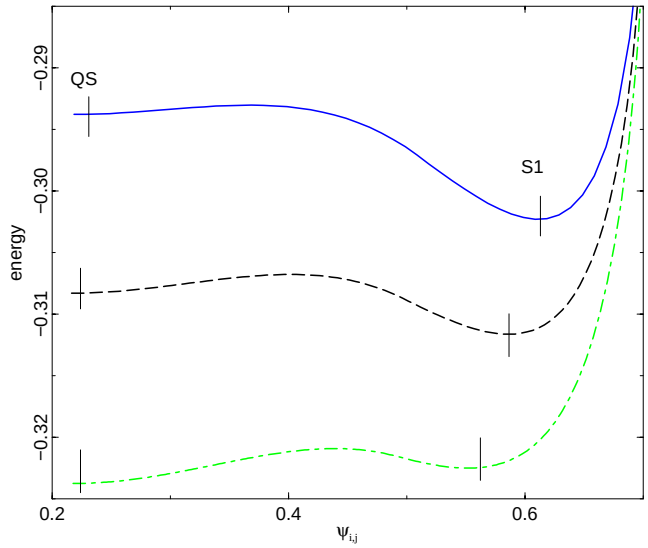

Fig. 9. Same as Figure 7 but for bipolaron (QS) with the constraint $\psi_{i,j} = c$ at $t = 0.08$, $U = 0.235$ (dotted-dashed line), $t = 0.075$, $U = 0.25$ (dashed line) and $t = 0.07$, $U = 0.26$ (full line), (Vertical lines indicates the location of the energy extrema corresponding to bipolaron (QS) and (S1).

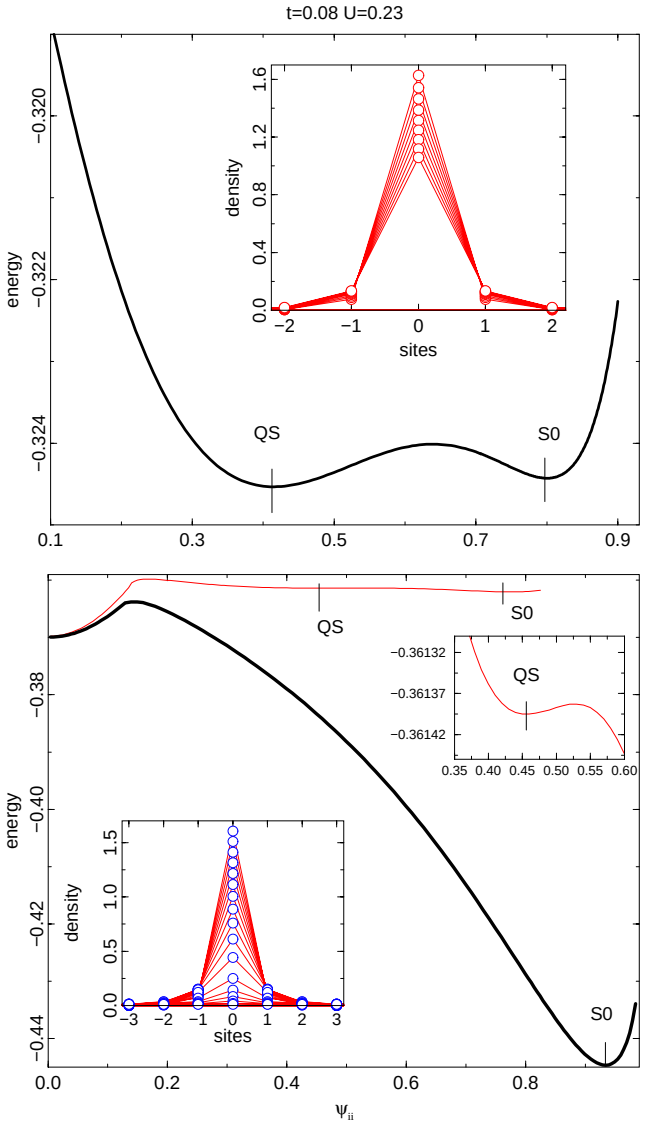

Fig. 10. Top: Radial PN energy barrier *versus* $\psi_{i,i} = c$ between (S0) and (QS) at $t = 0.08$, $U = 0.23$ Insert: Profile variation of the bipolaron electronic density along the same path. Bottom: Same at $t = 0.092$, $U = 0.1$ between bipolaron (S0) and the extended state at $\psi_{i,i} = 0$ (full line) and $t = 0.092$,$U = 0.204$ between bipolaron (S0), (QS) as an intermediate state and the extended state (thin line). Insert: Bipolaron profile (bottom left) and magnification of the (QS) region (top right).

have the same symmetry (see Fig. 10). We tested that it does not generate any path with a lower PN energy barrier when shifting the bipolaron (S0) or (QS) by one lattice spacing. For that, we compare the energy barrier obtained for shifting (S0) by one lattice spacing *via* the direct path (S1) $E_{\rm B}(\text{S0} \rightarrow \text{S1})$, to that obtained by the indirect path (S0) *via* (QS) and (S1) involving the jump of two consecutive barriers $E_{\rm B}(\text{S0} \rightarrow \text{QS})$ and $E_{\rm B}(\text{QS} \rightarrow \text{S1})$. We found that the energy barrier between (S0) and (QS) was always relatively too high to favor the indirect path.

When bipolaron (S1) becomes the ground-state, there are two PN energy barriers depending on the direction it is displaced, transversally or longitudinally. If it is displaced longitudinally in the direction of the bond (i, j) where (S1) is localized, the minimax may be obtained by varying the constraint $\psi_{j,k} = \psi_{k,j} = c$ which tends to displace (S1) longitudinally. Figure 11 shows this energy variation *versus* c starting from bipolaron (S1). The maximum along this path corresponds to the longitudinal star bisinglet bipolaron (BS). For $t = 0.03$ and $U > 0.28$, it costs less energy to use this path with minimax (BS′) than to use the path with minimax (S1/S0) passing by bipolaron (S0).

The transversal PN energy barrier of bipolaron (S1) can be also calculated. Actually, the transversal motion of (S1) with the lowest PN energy barrier has to be done in two steps (in the anti-integrable limit). If we denote by (i, j, k, l) the corner sites of an elementary square of the 2D lattice and move (S1) from the bond $i-j$ to bond $l-k$, then (S1) rotates once by $\pi/2$ around the center site i and again by $\pi/2$ but around the center site l. These two jumps have the same PN energy barrier. It can be measured from the height of the minimax determined by the constraint $\psi_{i,l} = \psi_{l,k} = c$. This path yields the 2 star multisinglet (BS′) with a diagonal symmetry axis where $\psi_{i,j} = \psi_{i,l}$ and where the two branches (i, j) and (i, l) are orthogonal. It is found that the longitudinal and transverse PN energy barrier are almost equal.

The precise determination of the PN energy barrier becomes more delicate close to the border line of the phase diagram Figure 2 with the domain of extended electrons. Here the binding energy of the bipolaron becomes very weak. To move a bipolaron, it may cost less energy to pass the energy barrier for breaking the pair of electrons (Fig. 10), producing extended electronic states, and next

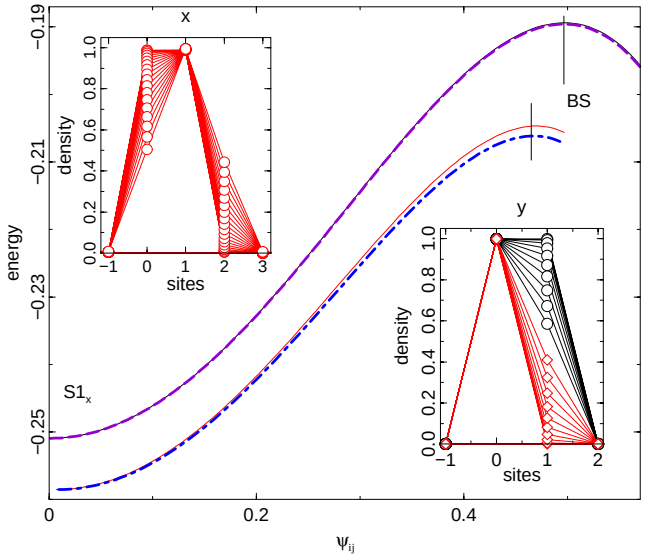

Fig. 11. Same as Figure 7 but for bipolaron (S1) moving in the longitudinal direction with the constraint $\psi_{j,k} = c$ or rotating transversally with the constraint $\psi_{i,l} = c$ at $t = 0.01$, $U = 0.3$ (upper lines), $t = 0.03$, $U = 0.3$ (lower lines). (Vertical lines indicates the location of the energy extrema corresponding to bipolaron (S1) and (BS) or (BS′)). Although almost the same, the curves for the transversal motion are slightly lower than those for the longitudinal motion. Insert: Variation of the profile of electronic density along the axis $i - j$ of bipolaron (S1) for the two continuous paths of the bipolaron at $t = 0.03$, $u = 0.3$ corresponding to the longitudinal motion (left top) and the transversal motion (right bottom).

to pass a new equivalent energy barrier for reconstructing the bipolaron at another site.

Figures 12 gather the resulting PN energy barrier *versus* U and for several values of t obtained by comparison of these different paths (for that reason we have broken lines with possible discontinuities). The essential result is that close to the region of the triple point between bipolaron (S0), (S1) and (QS), the Peierls-Nabarro energy barrier sharply drops and reaches the same order of magnitude as the binding energy of the bipolarons. When U slightly increases beyond this point, the binding energy of the bipolaron sharply decreases. Conversely, when U slightly decreases, the PN energy barrier sharply increases. In that region, the paths allowing a shift by one lattice spacing of a bipolaron with the smallest PN energy barrier involves the successive transformations ... (QS) → (S1) → (QS) ...

There are regions in the parameter space where the bipolaron binding energy becomes very small, for example when t is small and $U > 1/4$) (*e.g.* Fig. 12 at $t = 0.03$). The PN energy barrier of a bipolaron is then practically equal to the PN energy barrier of a free single polaron. In other regions, close to the first-order transition border line with the extended states, the bipolaron binding energy also becomes very small, but then the PN energy barrier is practically that which has to be overcome for the electron delocalization.

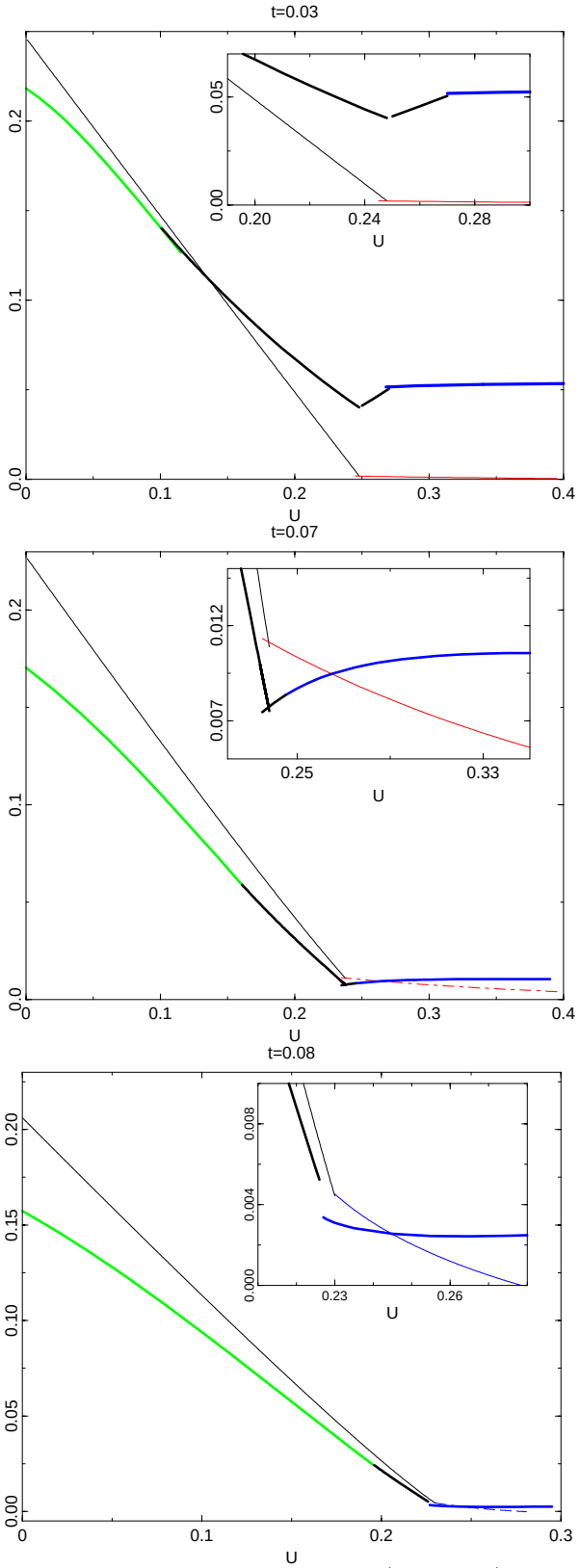

Fig. 12. Peierls-Nabarro energy barrier (thick lines) and Binding energy (thin lines) of ground-state bipolarons *versus* U for different values of t: $t = 0.03$ (top), $t = 0.07$ (middle) and $t = 0.08$ (bottom). The lines are broken because of the change of minimax. Inserts: magnification in the region of first order transition.

6 Concluding remarks

The interplay between the electron-phonon coupling and the direct electronic repulsion has been treated accurately in the adiabatic Holstein-Hubbard model in two dimensions. Numerical investigations complemented by analytic variational calculations yield the phase diagram of the ground-state of a single bipolaron, which consists of several domains separated by first order transition lines (see Fig. 2). It is found that the different bipolaronic states that are obtained, already exist at the anti-integrable limit and can be generated from this limit by continuation.

There is an interesting region in the phase diagram where the bipolaronic ground-state becomes a quadrisinglet bipolaron, which is a superposition of four singlets sharing one central site. The binding energy of that bipolaron is the result of the spin resonance between a strongly localized polaron and a peripheral electron localized on its nearest neighbors.

There is a triple point where the three kinds of bipolaron coexist with the same binding energy, which is still significantly large and non-negligible. The internal modes of the bipolarons soften significantly in that region. Moreover, the Peierls-Nabarro energy barrier (PN) of the bipolaron in that region is strongly depressed, which improves the classical mobility of this bipolaron. This effect is related to the appearance of several intermediate metastable bipolaronic state which have almost the same energy. A small variation of parameters (U, t) in that region suffices either to lift the near degeneracy, with a PN energy barrier which grows very fast, or to depress sharply the binding energy of the bipolaron itself. The energy landscape around the bipolaron has been explored. It has been found that it is quite flat in the region of the triple point with several minimum energy states close in energy and small energy barriers between them.

These features strongly support the conjecture that the quantum tunneling of the bipolaron will be strongly enhanced in the vicinity of this triple point due both to the small PN energy barrier and to the hybridization between the nearly degenerate states. This assertion will be confirmed by the results of the next paper where the quantum lattice fluctuations will be treated as perturbation through a tight binding model [17].

Unlike the conclusion of reference [11], we find a plausible mechanism for a drastic reduction, under specific conditions by several orders of magnitude, of the effective mass of a bipolaron while preserving a relatively large binding energy. Let us recall that Figure 4 shows that the binding energy close to the triple point is still about $0.005E_0$. Since $E_0 = 8g^2/\hbar\omega_0$ could reach in some realistic physical models a magnitude of about 10 eV, this binding energy can be close to 0.05 eV which corresponds in temperature units to 500 K! In the same region, the Peierls-Nabarro energy barrier has a value almost equal to this binding energy. It is drastically reduced compared to what could be expected for small bipolarons in standard theories. Note that is about 50 times smaller than the Peierls-Nabarro energy barrier of the bipolaron (S0) at $U = 0$ and the same value of t.

When the temperature of the system goes below this characteristic temperature where bipolarons can form, and if the tunnelling energy could reach comparable values (which will be shown in the next paper), this effect might be sufficient to favor a superfluid state at 0 K against either a bipolaron ordering or a magnetic polaron ordering. This state could persist to unusually large temperatures. There is, of course, another condition, which is that the direct bipolaron interactions are not too strong. This is very unlikely to be true at half-filling, where the polarons are close-packed, but this condition might become fulfilled when the density of electrons moves sufficiently far from half-filling. These quantitative results in the Holstein-Hubbard model yield a more quantitative support to earlier but less specific conjectures that high T_c superconductivity could be explained by a well balanced competition between electron-electron repulsion and electron-phonon interaction [15,16].

The methods used above should also work with other perturbations from the anti-integrable limit. In the present paper, the Laplacian form for the kinetic energy implies that the bipolaron ground-state when it has the square symmetry, has necessarily the trivial quantum symmetry (s). However, it is not physically unrealistic to assume that the electronic kinetic energy terms in Hamiltonian (1) might be different from a discrete Laplacian form[4]. When there are second-nearest-neighbor electronic transfers with significant amplitudes (but not necessarily as large as the nearest-neighbor integral) and with appropriate signs, the ground-state electronic wave function $\{\psi_{i,j}\}$ of bipolaron (QS) should have a (d) symmetry (see Appendix C). A superfluid state of such bipolarons with a degenerate internal quantum symmetry could be perhaps related with the now well accepted fact that the superconducting order parameter of cuprates has a (d) wave symmetry [29]. Further works will investigate consequences of this quantum symmetry. We expect that when the (d) wave symmetry is favored by appropriate terms, the stability domain of the bipolarons that can take advantage of this symmetry will be extended: that is, those of bipolaron (QS).

In principle, the method used in this paper for calculating adiabatic bipolarons could be extended to more complex and realistic models. There are many kinds of bipolarons in the anti-integrable limit, as shown in Appendix A. It is not obvious that only bipolarons (S0), (S1) or (QS) are competing as ground-states. More generally, if there are more transfer integrals between further neighbors, other N_2 star multisinglets with $N_2 > 4$ (*e.g.* $N_2 = 8$ etc.) might become more favorable as bipolaron ground-state in some cases.

Of course, the present study with only two electrons is by far not sufficient to describe real cuprates where the density of electrons is close to half filling. Our model suffers in that we are not yet able to describe in a satisfactory fashion the interactions between the bipolarons. Nevertheless, we believe that we already obtained useful

[4] A reduced Holstein-Hubbard Hamiltonian on the copper square 2D sublattice of cuprates should involve more than nearest-neighbor transfer integral due to the oxygen bridges.

informations on the effect of competing strong electron-phonon and strong electron-electron interactions. Our approach supports the possibility of a bipolaronic mechanism to explain high T_c cuprate superconductors, and this might be a clue for a more consistent explanation for the origin of high T_c superconductivity in real high T_c superconducting cuprates.

Of course, one may argue against our approach that assuming a large tunnelling energy for bipolarons is a warning that the system might not be well described anymore by perturbative methods from the adiabatic limit. But, our results also warn that perturbative methods from a Fermi liquid model with strong electron interactions is also quite far from its limit of validity because of the non-negligible lattice distortions that could be generated. From a strict mathematical point of view, there are no reasons why the same physical state could be not described from different limits, so that a debate about this question of principle is useless. In the end, only the efficiency and simplicity of a theory, are the right criteria for physicists.

We thank R.S. MacKay and C. Baesens for useful discussions. One of us (LP) acknowledges DAMTP in Cambridge for its hospitality during the completion of this manuscript.

Appendix A: Bipolaron states at the anti-integrable limit

We describe an elementary classification of the bipolaron solutions in the anti-integrable limit. It could also probably be obtained as a special case of two electrons of the more sophisticated homology theory that was recently developed by Baesens and MacKay [30] for the pure Holstein model with many electrons.

These bipolaron solutions $\{\psi_{i,j}\}$ fulfill equations (10, 13) at $t = 0$, which yields

$$\left(-\frac{1}{4}(\rho_i + \rho_j) + U\delta_{i,j}\right)\psi_{i,j} = F_{\rm el}\psi_{i,j} \qquad \text{(A.1)}$$

where the electronic density ρ_i is defined by equation (12).

We first note that for any solution of this equation, the phases of the complex numbers $\psi_{i,j}$ can be chosen arbitrarily and independently. Thus, in this paper, we remove this trivial degeneracy by choosing their phases to be zero, that is $\psi_{i,j}$ is assumed to be real positive. However, it could be removed by fixing another symmetry for the bipolaron (*e.g.* symmetry (s') or (d)). In principle, removing the phase degeneracy is necessary to allow a unique continuation of a solution at $t \neq 0$ (if there is no other continuous degeneracy). Since we noted that the bipolaron ground-state at $t \neq 0$ necessarily fulfills this condition, it could be found among these continued solutions. Actually, this trick is analogous to that used in reference [25] for proving the existence of discrete breathers.

There is another trivial degeneracy at $t = 0$ but that is now discrete. Any solution of equation (A.1) yields infinitely many other solutions with the same energy, which are simply obtained by arbitrary permutations of the sites of the lattice $j = \mathcal{P}(i)$.

For each solution, the set of occupied sites $i \in \mathrm{S}$ is defined by the condition $\rho_i \neq 0$. We call *link* a pair of sites (i, j) such that $\psi_{i,j} \neq 0$ (which implies $i \in \mathrm{S}$ and $j \in \mathrm{S}$). A bipolaron state at $t = 0$ is said to be connected if the graph generated by all the links is connected.

We first investigate the connected states of equation (A.1), which implies that when $\psi_{i,j} \neq 0$,

$$U\delta_{i,j} - \frac{1}{4}(\rho_i + \rho_j) = F_{\rm el}. \qquad \text{(A.2)}$$

$F_{\rm el}$ is independent of the pair of connected sites (i, j). Considering two different sites i and j connected to a third site n, it comes out that $\rho_i + \rho_n = \rho_j + \rho_n$, which implies $\rho_i = \rho_j$. More generally, two occupied sites connected by some path with an even number of links have necessarily the same electronic density. As a result, the set of occupied sites S is the union of two disjoint sets of sites S_1 and S_2 where the electronic densities are the same. For $i \in \mathrm{S}_1$, the electronic density is $\rho_i = \rho_1$ and for $j \in \mathrm{S}_2$, $\rho_j = \rho_2$. Moreover, sites $i \in \mathrm{S}_1$ are only linked to sites $j \in \mathrm{S}_2$ and *vice versa*.

We consider separately the connected bipolaron states without and with doubly occupied sites i. These sites are defined by the condition $\psi_{i,i} \neq 0$.

A.1 Connected bipolaron states with no doubly occupied site

If $\psi_{i,i} = 0$ for any i, the electronic wave function is a normalized combination of two sites singlet states defined in equation (18), and consequently these states and their energies do not depend on U.

$N_{\rm s} = N_1 + N_2$ is defined as the total number of occupied sites, N_1 is the number of sites in S_1 with density ρ_1 and N_2 the number of sites in S_2 with density ρ_2. Since the total number of electrons is two,

$$N_1\rho_1 + N_2\rho_2 = 2. \qquad \text{(A.3)}$$

It follows from equation (14) that

$$F_{\rm v} = -\frac{1}{8}\sum_i \rho_i^2 = -\frac{1}{8}(N_1\rho_1^2 + N_2\rho_2^2) \qquad \text{(A.4)}$$

and equivalently from equations (16, A.2)

$$F_{\rm v} = -\frac{1}{4}(\rho_1 + \rho_2) + \frac{1}{8}(N_1\rho_1^2 + N_2\rho_2^2). \qquad \text{(A.5)}$$

Identifying the two results (A.4, A.5), and using equation (A.3), two solutions come out which are first

$$\rho_1 = \frac{1}{N_1} \quad \text{and} \quad \rho_2 = \frac{1}{N_2} \quad \text{with} \qquad \text{(A.6)}$$

$$F_{\rm v} = -\frac{N_{\rm s}}{8N_1N_2} \qquad \text{(A.7)}$$

and second

$$\rho_1 = \rho_2 = \frac{2}{N_\mathrm{s}} \quad \text{with} \tag{A.8}$$

$$F_\mathrm{v} = -\frac{1}{2N_\mathrm{s}}\cdot \tag{A.9}$$

In the first case (A.6), we have $\rho_1 \neq \rho_2$ when $N_1 \neq N_2$. Then $\psi_{i,j} \neq 0$ when $i \in \mathrm{S}_1$ and $j \in \mathrm{S}_2$ or *vice versa*. This condition determines a rectangular $N_1 \times N_2$ matrix. The square of its real positive coefficients fulfills the linear equations (12)

$$\sum_{j\in \mathrm{S}_2} \psi_{i,j}^2 = \frac{1}{2N_1} \tag{A.10}$$

$$\sum_{i\in \mathrm{S}_1} \psi_{i,j}^2 = \frac{1}{2N_2}\cdot \tag{A.11}$$

A particular solution of this set of equations is $\psi_{i,j}^2 = 1/(2N_1N_2)$. However, there are $N_1 + N_2$ linear equations to determine the N_1N_2 coefficients. Except for the case $N_1 = 1$ or equivalently $N_2 = 1$, (we have $N_1 \neq N_2$), this solution $\psi_{i,j}$ is degenerate and belongs to a nonvoid bounded and compact domain defined by the positivity of $\psi_{i,j}^2$.

The solutions with $N_1 = 1$ appear especially interesting, not only because they are not continuously degenerate but because their energy $F_\mathrm{v} = -(N_2+1)/(8N_2) < -1/8$ is significantly lower than zero. It is not far above those of the bipolaron (S0) which is $F_\mathrm{v} = -1/2+U$ and those of the singlet bipolaron (S1) which is $F_\mathrm{v} = -1/4$ (see Fig. 13). We call them star multisinglets. (S1) and (QS) are star multisinglets with $N_2 = 1$ and $N_2 = 4$ (see Fig. 1).

In the second case (A.8) or in the first case when $N_1 = N_2$, the electronic densities at the $N_\mathrm{s} = 2N_1$ occupied sites are equal. Then there are in general $N_\mathrm{s}(N_\mathrm{s}-1)/2$ nonzero coefficients $\psi_{i,j} = \psi_{j,i}$ since there are no doubly occupied sites ($\psi_{i,i} = 0$). They fulfill N_s equations $\sum_j \psi_{i,j}^2 = 1/(2N_\mathrm{s})$ (12). Again, this system has a trivial solution, which is $\psi_{i,j}^2 = 1/(2N_\mathrm{s}(N_\mathrm{s}-1))$ for $i \neq j \in \mathrm{S}$. However, when $N_\mathrm{s} \geq 4$, this system of equations becomes underdetermined and yields continuously degenerate solutions that belong to a compact domain since again $\psi_{i,j}^2$ must be found positive.

It is worthwhile to remark that although these solutions were assumed to be connected, when they form a continuously degenerate set this set may contain non-connected states just at the border of the compact domain of solutions. For example, in this second case, let us split the set S of occupied sites in two disjoint subsets T_1 and T_2 with $M_\mathrm{s} \geq 2$ and $N_\mathrm{s} - M_\mathrm{s} \geq 2$ sites respectively. Let us set $\psi_{k,l} = \psi_{l,k} = 0$ for $k \in \mathrm{T}_1$ and $l \in \mathrm{T}_2$, which corresponds to $M_\mathrm{s}(N_\mathrm{s} - M_\mathrm{s})$ conditions. When $N_\mathrm{s}(N_\mathrm{s}-1)/2 - M_\mathrm{s}(N_\mathrm{s}-M_\mathrm{s}) \geq N_\mathrm{s}$, the equation $\sum_j \psi_{i,j}^2 = 1/N_\mathrm{s}$ has the solution $\psi_{i,j} = 1/\sqrt{(M_\mathrm{s}-1)N_\mathrm{s}}$ for $i \neq j \in \mathrm{T}_1$ and $\psi_{i,j} = 1/\sqrt{(N_\mathrm{s}-M_\mathrm{s}-1)N_\mathrm{s}}$ for $i \neq j \in \mathrm{T}_2$. This situation is found to occur for $N_\mathrm{s} \geq 6$.

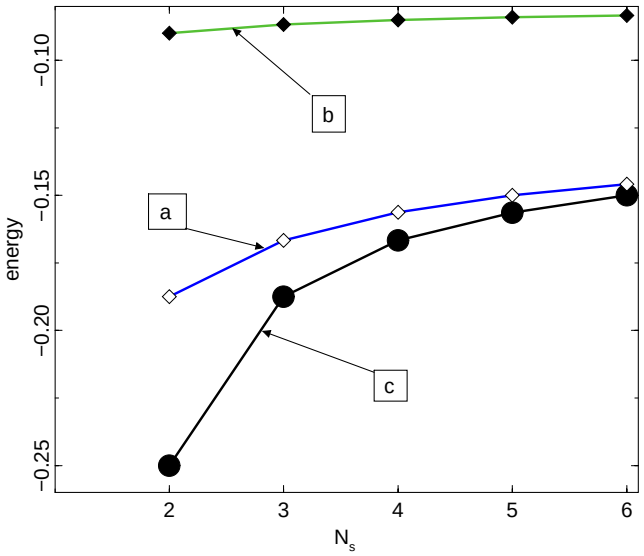

Fig. 13. At $t = 0$, energy as a function of N_s: (a) star sisters solutions for $U = 0.25$, (b) star sisters solutions $U = 0.4$, and (c) star multisinglets (S1) for $N_\mathrm{s} = 2$, bisinglet (BS) for $N_\mathrm{s} = 3$, trisinglet (TS) for $N_\mathrm{s} = 4$, quadrisinglet (QS) for $N_\mathrm{s} = 5$.

A.2 Connected bipolaron states with doubly occupied sites at U ≠ 0

Let us require $N_\mathrm{s} > 1$ to avoid the onsite bipolaron (S0). Such connected solutions $\{\psi_{i,j}\}$ of equation (A.1) have at least one doubly-occupied site k (*i.e.* such that $\psi_{k,k} \neq 0$). The set of occupied sites can be split in two sets S_1 and S_2 with electronic density ρ_1 and ρ_2, respectively. Let us consider a doubly occupied site k which we assume to belong to the set of sites S_1 with electronic density ρ_1. Let us also consider a site $l \in \mathrm{S}_2$ such that $\psi_{k,l} \neq 0$. There exists such a site since the solution is connected. Then, because of equation (A.2), we have

$$\begin{aligned} F_\mathrm{el} &= -\frac{1}{2}\rho_k + U = -\frac{1}{4}(\rho_k + \rho_l) \\ &= -\frac{1}{4}(\rho_1 + \rho_2) = -\frac{1}{2}\rho_1 + U \end{aligned} \tag{A.12}$$

which implies

$$U = \frac{\rho_1 - \rho_2}{4}\cdot \tag{A.13}$$

All the doubly occupied sites must belong to S_1. The nonzero Hubbard amplitude U obviously implies distinct electronic density for doubly-occupied and non-doubly-occupied sites. It follows from equation (A.3) that

$$\rho_1 = 2\frac{1+2UN_2}{N_\mathrm{s}} \quad \text{and} \quad \rho_2 = 2\frac{1-2UN_1}{N_\mathrm{s}} \tag{A.14}$$

which implies

$$-\frac{1}{2N_2} < U < \frac{1}{2N_1} \tag{A.15}$$

in order that both ρ_1 and ρ_2 be positive.

We now obtain from equations (14, 16) at $t = 0$

$$F_{\rm v} = \frac{1}{8}(N_1\rho_1^2 + N_2\rho_2^2) - \frac{1}{4}(\rho_1 + \rho_2) \tag{A.16}$$

and substituting (A.14) in (A.16)

$$F_{\rm v} = \frac{1}{2N_{\rm s}}[4U^2 N_1 N_2 + 2U(N_1 - N_2) - 1] \tag{A.17}$$

According to equation (12), the set of electronic states $\psi_{i,j} = \psi_{j,i}$ satisfy

$$\frac{\rho_1}{2} = \psi_{i,i}^2 + \sum_{j\in {\rm S}_2} \psi_{i,j}^2 \quad \text{for} \quad i \in {\rm S}_1 \tag{A.18}$$

$$\frac{\rho_2}{2} = \sum_{i\in {\rm S}_1} \psi_{i,j}^2 \quad \text{for} \quad j \in {\rm S}_2 \tag{A.19}$$

where ρ_1 and ρ_2 are given by equations (A.14). There are $N_1 + N_2$ linear equations for calculating $N_1(N_2 + 1)$ positive numbers $\psi_{i,i}^2$ with $i \in {\rm S}_1$ and $\psi_{i,j}^2 = \psi_{j,i}^2$ with $i \in {\rm S}_1$ and $j \in {\rm S}_2$. A particular solution is obtained when all $\psi_{i,j}^2 = \rho_2/(2N_1) = (1 - 2UN_1)/(N_{\rm s}N_1)$ and all $\psi_{i,i}^2 = (N_1\rho_1 - N_2\rho_2)/(2N_1) = (N_1 - N_2 + 4UN_1N_2)/(N_1N_2)$. The positivity of $\psi_{i,i}^2$ requires

$$\frac{N_2 - N_1}{4N_1N_2} < U. \tag{A.20}$$

Actually, there are no positive solutions at all to equations (A.18, A.19) when this condition is not fulfilled.

When conditions (A.15) and (A.20) are fulfilled and when $N_1 > 1$, the number of variables exceeds the number of equations, and there is a compact set of degenerate positive solutions to the linear equations (A.18, A.19).

When $N_1 = 1$ and when

$$\frac{N_2 - 1}{4N_2} \le U \le \frac{1}{2} \tag{A.21}$$

there is a unique solution to this set of linear equations. For a given $N_{\rm s}$, it has the lowest energy $F_{\rm v}$ (plotted in Fig. 13 for different values of U). This solution is called N_2 star sister. It can be interpreted as a mixing between the bipolaron (S0) and the N_2 star multisinglet. We denote (S0/S1) the one star sister that mixes both (S0) and (S1) etc. According to the implicit function theorem, this nondegenerate solution can be continued to t nonzero except at the bifurcation points at $U = 1/2$ and $U = (N_2 - 1)/4N_2$ where this solution bifurcates with (S0) and the N_2 star multisinglet, respectively. In the anti-integrable limit $t = 0$, its energy is larger than both those of (S0) and N_2 multisinglet (see part 5 for $t > 0$).

A.3 Non connected bipolaron states

Let us now assume that we have a solution $\{\psi_{i,j}\}$ of equation (A.1), which is not connected. Then, it can be decomposed into a sum of normalized connected components $\{\psi_{i,j}^\alpha\}$. We define ${\rm S}_\alpha$ as a set of lattice sites that are connected with each other by a sequence of links. $\psi_{i,j}^\alpha \neq 0$ is proportional to $\psi_{i,j}$ for $i \in {\rm S}_\alpha$ and $j \in {\rm S}_\alpha$ and zero elsewhere. The proportionality coefficient λ_α is chosen in order that $\{\psi_{i,j}^\alpha\}$ normalized. Then we have

$$\psi_{i,j} = \sum_\alpha \lambda_\alpha \psi_{i,j}^\alpha \tag{A.22}$$

with

$$\sum_\alpha |\lambda_\alpha|^2 = 1. \tag{A.23}$$

Two components α and β have no common occupied site.

Then, $\{\psi_{i,j}^\alpha\}$ is a connected solution of equation (A.1), for the eigenenergy $F_{\rm el}^\alpha = F_{\rm el}/|\lambda_\alpha|^2$ and the Hubbard term $U_\alpha = U/|\lambda_\alpha|^2$.

If component α has no doubly occupied sites, it does not depend on U. Then if $N_1^\alpha + N_2^\alpha = N_{\rm s}^\alpha$ represents the number of sites in each of the two groups of sites with different electronic densities defined at the beginning of this Appendix, equation (A.2) implies

$$|\lambda_\alpha|^2 = -4F_{\rm el}\frac{N_1^\alpha N_2^\alpha}{N_{\rm s}^\alpha} \tag{A.24}$$

If component α has doubly occupied sites (see Appendix A.2), then equation (A.1) implies

$$|\lambda_\alpha|^2 = -N_{\rm s}^\alpha F_{\rm el} - U(N_2^\alpha - N_1^\alpha) \tag{A.25}$$

There are constraints for solving the second equation because of inequalities (A.15) and (A.20), which imply

$$-\frac{1}{2N_2^\alpha} < \frac{U}{|\lambda_\alpha|^2} < \frac{1}{2N_1^\alpha} \tag{A.26}$$

$$\frac{N_2^\alpha - N_1^\alpha}{4N_1^\alpha N_2^\alpha} < \frac{U}{|\lambda_\alpha|^2}. \tag{A.27}$$

Conversely, we can construct non-connected bipolaron states which are combination of non-overlapping connected states. Then the amplitude $|\lambda_\alpha|^2$ is defined by equations (A.24) or (A.25), but then we have to choose $F_{\rm el}$ in order that the normalization condition (A.23) is fulfilled. This is easy to do when only components α with no doubly occupied sites are involved. Otherwise, we have to take into account the constraints (A.15) and (A.20). There are many such solutions but we did not investigate them in detail. Some of them are easy to find: for example, the nonconnected solution with two components involving the bipolaron (S0) located on two adjacent sites. This solution is called (2S0) and has the energy $U - 1/4$.

It can be checked that the energy of the disconnected state is always larger than those of its components with the smallest energy.

Appendix B: Two-site model

It is instructive to analyze all the extrema of the variational form (14) on a lattice reduced to only two sites i and j, because it can be explicitly calculated in all detail.

However, a limitation of this restricted model is that in addition to the absence of extended states, the bipolaron (QS) cannot occur with only two sites.

Setting $\psi_{i,i} = x$, $\psi_{j,j} = y$ and $\psi_{i,j} = z$, using the normalization $x^2 + y^2 + 2z^2 = 1$, (14) becomes

$$F_v = -\frac{1}{4} - \frac{1}{4}(x^2 - y^2)^2) + U(x^2 + y^2) \\ -\sqrt{2}t(x+y)\sqrt{1 - x^2 - y^2}. \qquad \text{(B.1)}$$

Considering as equivalent the extrema obtained by symmetries ($x \to -x$, $y \to -y$) and ($x \to y$, $y \to x$), there are up to 4 kinds of extrema to this variational form at $t = 0$:

- Bipolaron (S0) with energy $U - 1/2$ is a local minimum for $U < 1/2$ and becomes a saddle point with only one unstable direction for $U > 1/2$. There are two symmetric such solutions located either at site i or at site j.
- Bipolaron (S1) with energy $-1/4$ is a local minimum for $U > 0$ and becomes a maximum (with two unstable directions) for $U < 0$.
- Bipolaron (2S0) is a non connected state consisting of $\psi_{i,i} = \psi_{j,j} = 1/\sqrt{2}$ and $\psi_{i,j} = \psi_{j,i} = 0$. It is a maximum (two unstable directions) for $U > 0$ and a saddle point (one unstable direction) for $U < 0$.
- When $0 < U < 1/2$, there is another extremum which is the 1 star sister (S1/S0) described in Appendix A. It is a saddle point with one unstable direction. It bifurcates with bipolaron (S1) at $U = 0$ and with bipolaron (S0) at $U = 1/2$. There are two symmetric such solutions located at site i or j.

The minimax corresponding to the PN energy barrier for moving either bipolaron (S0) or (S1) is nothing but the unique saddle point which could be (2S0) ($U < 0$), (S1/S0) ($0 < U < 1/2$) or (S1) ($1/2 < U$).

At $t = 0$ and $U = 0$, bipolarons (S1) and (2S0), which are both spatially symmetric, have also the same energy and the same electronic density (see Fig. 14). When $t \neq 0$, this degeneracy is raised as shown in Figure 14.

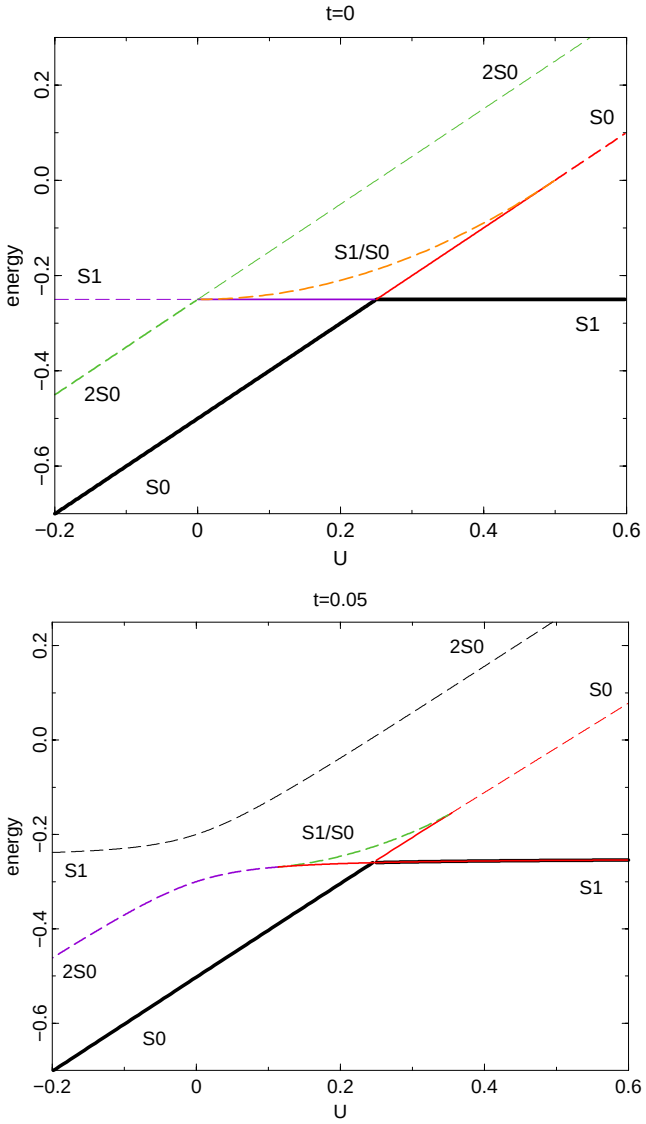

Fig. 14. Bipolaron energies *versus* U at the anti-integrable limit $t = 0$ (top) and at $t = 0.05$ (bottom). Ground-state (thick full line), stable bipolaron (full line), minimax (thick dashed line), maximum (thin dashed lines).

Appendix C: Quantum symmetries of bipolarons

Eventhough no nontrivial quantum symmetry appears for the bipolaronic ground-states of our model, it is worthwhile to going forward now some further work of ours and discuss the possibility of nontrivial quantum symmetries. Actually, such symmetries are already *latent* in the anti-integrable limit and could be manifested easily in appropriately modified models.

As we pointed out, in the anti-integrable limit, only the modulus of $\psi_{m,n}$ is determined but not the phases. This degeneracy is expected to be lifted by the perturbation from this limit due the electronic kinetic energy. However, it might not be completely lifted in some cases.

This situation may occur for bipolarons associated with a lattice distortion (or equivalently an electronic density) which has the square symmetry of the lattice (group C_{4v}). This symmetry group has only two generators, which are for example the $\pi/2$ rotation and the reflection with respect to the x axis. Any of the symmetry transformations change only the phase of the electronic wave function $\{\psi_{m,n}\}$ but not its modulus $|\psi_{m,n}|$.

There are three possible group representations for C_{4v} usually denoted A, B and E in textbooks of crystallography [31]. We denote them (s), (s') and (d) respectively[5]. (see Fig. 15)

[5] In principle, the (d) symmetry characterizes the dimension 5 representation $l = 2$ of the continuous rotation group $O(3)$ in three dimensions. We still use this terminology for the symmetry group of the square lattice although it is not appropriate, but because it is the most standard one in symmetry theory of superconductivity.

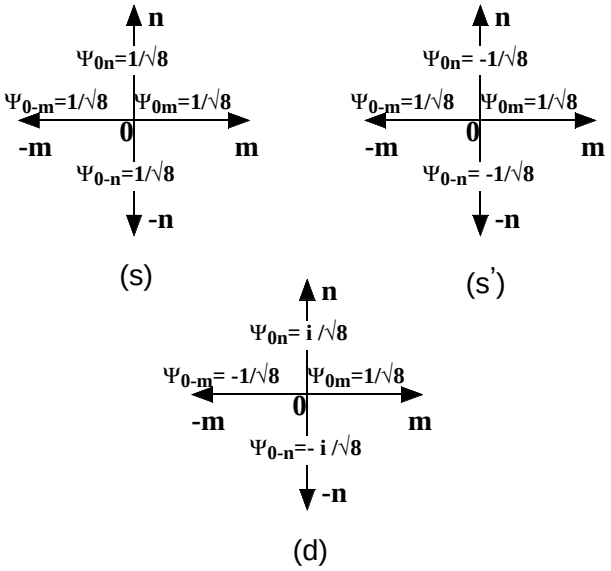

Fig. 15. Three (QS) bipolarons at the anti-integrable limit with the different quantum symmetries (s) (top left), (s') (top right) and (d) (bottom).

- When $\{\psi_{m,n}\}$ has the (s) symmetry, it is unchanged by any symmetry operation. This representation has obviously dimension 1.
- When $\{\psi_{m,n}\}$ has the (s') symmetry, $\{\psi_{m,n}\}$ is changed into $\{-\psi_{m,n}\}$, by a $\pi/2$ rotation of the lattice. It is unchanged by reflection with respect to the x axis. The other transformations are obtained by combinations of these ones. This representation has also dimension 1.
- For the (d) symmetry, $\{\psi_{m,n}\}$ is changed into $\{i\psi_{m,n}\}$, by a $\pi/2$ rotation of the lattice and $\{\psi_{m,n}\}$ is changed into $\{\psi^*_{m,n}\}$, by reflection with respect to the x axis. This representation has dimension 2.

We now note that, in the anti-integrable limit, bipolaron (S0) always has the symmetry (s). For bipolaron (S1), which does not have the square symmetry but only an axis of symmetry, the symmetry is too poor to generate a d symmetry. Bipolaron (QS) is more interesting because it has the square symmetry for its electronic density but its quantum wave function may have three different quantum symmetries (s), (s') and (d) respectively (see Fig. 15). These three states are degenerate in the anti-integrable limit but the electronic kinetic energy lifts this degeneracy. For a Laplacian-like kinetic energy as in the model treated where $t > 0$ in (6), the preferred quantum symmetry is (s). However, symmetry (d) can be easily favored when there are next nearest-neighbor transfer integrals with negative signs in the electronic kinetic energy.

In summary, we described in Appendices A and C a systematic method that allows one to construct all the possible bipolaron solutions existing at the anti-integrable limit $t = 0$. There are bipolaron states with no continuous degeneracy and others with a continuous degeneracy. Bipolarons (S0) and star multisinglets with N_2 small appear to be the best candidates for bipolaronic ground-states when the electronic kinetic energy is switched to be non-zero. Star sisters may appear as minimaxes but are not found as ground-states. There are bipolarons with the square lattice symmetry (for example (QS)) which may have nontrivial quantum symmetries (s') or (d) instead of (s).

References

1. J. Bardeen, L.N. Cooper, J.R. Schrieffer, Phys. Rev. **106**, 162–164 (1957); **108**, 1175–1204 (1957).
2. A.B. Migdal, Zh. Eksperim. Fiz. **34**, 1438 (1958); Sov. Phys.-JETP **7**, 996 (1958).
3. W.L. McMillan, Phys. Rev. **167**, 331 (1968).
4. J.G. Bednorz, K.A. Müller, Z. Phys. B **64**, 1796 (1986).
5. K.A. Müller, G. Benedek, *Phase Separations in Cuprate Superconductors* (World Scientific Pub., the Science and Culture series, 1993).
6. J.R. Waldram, *Superconductivity of Metals and Cuprates* (IOP Publishing Ltd, 1996).
7. A.S. Alexandrov, E.K.H. Salje, W.H. Liang, *Polarons and Bipolarons in High T_c Superconductors and related Materials* (Cambridge University Press, 1995).
8. L. Landau, Phys. Z. Sowjetunion **3**, 664 (1933).
9. A.S. Alexandrov, J. Ranninger, S. Robaszkiewicz, Phys. Rev. B **33**, 4526–4552 (1986).
10. D. Emin, T. Holstein, Phys. Rev. Lett. **36**, 4526 (1976); D. Emin, Phys. Today (june 1982), pp. 34.
11. B.K. Chakraverty, J. Ranninger, D. Feinberg, Phys. Rev. Lett. **81**, 433–436 (1998).
12. S. Aubry, P. Quemerais, in *Low Dimensional Electronic Properties of Molybdenum Bronzes and Oxides*, edited by C. Schlenker (Kluwer, Academic Publishers Group, 1989), pp. 295–405.
13. S. Aubry, G. Abramovici, J.L. Raimbault, J. Stat. Phys. **67**, 675–780 (1992).
14. S. Aubry, J. Phys. France IV **3**, C2–349 (1993).
15. S. Aubry in reference [5], 304–334.
16. S. Aubry in reference [7], 271–308.
17. L. Proville, S. Aubry (in preparation).
18. L. Proville, *Structures polaroniques et bipolaroniques dans le modèle de Holstein Hubbard adiabatique à deux électrons et ses extensions* (Ph.D thesis, University Paris XI, 1998).
19. L. Proville, S. Aubry, Physica D **113**, 307–317 (1998).
20. S. Aubry, Physica D **86**, 284–296 (1995).
21. G. Kalosakas, S. Aubry, G. Tsironis, Phys. Rev. B **58**, 3094–3104 (1998).
22. P.Y. Le Daëron, *Transition Metal-Isolant dans les chaines de Peierls* (Ph.D thesis, University Paris XI, 1983).
23. J.L. Marín, S. Aubry, Nonlinearity **9**, 1501–1528 (1997).
24. C. Baesens, R.S. MacKay, Nonlinearity **7**, 59–84 (1994).
25. R.S. MacKay, S. Aubry, Nonlinearity **7**, 1623–43 (1994).
26. P.W. Anderson, G. Baskaran, Z. Zou, T. Hsu, Phys. Rev. Lett. **58**, 2790–2793 (1987).
27. S. Aubry, T. Cretegny, Physica D **119**, 34–46 (1998).
28. T. Cretegny, Ph.D thesis, ENS Lyon, 1998; T. Cretegny, S. Aubry (in preparation).
29. D. Pines, Physica C **282**, 273–278 (1997).
30. C. Baesens, R. MacKay, J. Phys. A: Math. Gen. **31**, 10065–10085 (1998).
31. *Spectres de vibration et symétrie des cristaux*, H. Poulet, J-P. Mathieu, edited by Gordon and Breach (Paris, 1970).